SIRT1's O-GlcNAcylation protects cold exposed-induced skeletal muscle damage through ameliorates mitochondrial homeostasis

Yu Cao
Heilongjiang Bayi Agricultural University https://orcid.org/0000-0001-7387-8349
Meng Zhang
Heilongjiang Bayi Agricultural University
Ye Li
Heilongjiang Academy of Agricultural Sciences
Jing-Jing Lu
Heilongjiang Bayi Agricultural University
Wan-Hui Zhou
Heilongjiang Bayi Agricultural University
Xiao-Shuag Li
Heilongjiang Bayi Agricultural University
Hao Shi
Virginia Polytechnic Institute and State University
Bin Xu (xubin@byau.edu.cn)
https://orcid.org/0000-0002-9395-3606
Shi-Ze Li
Heilongjiang Bayi Agricultural University

Research

Keywords: Cold stress, Skeletal muscle, Metabolic homeostasis imbalance, SIRT1, O-GlcNAcylation

Posted Date: June 21st, 2022

DOI: https://doi.org/10.21203/rs.3.rs-1725313/v1

SIRT1's O-GlcNAcylation protects cold exposed-induced skeletal muscle damage through ameliorates mitochondrial homeostasis

Yu Cao[1,4], Meng Zhang[1,4], Ye Li[2], Jing-Jing Lu[1], Wan-Hui Zhou[1], Xiao-Shuang Li[1], Hao Shi[3], Bin Xu[1,**], Shi-Ze Li[1,*]

[1]College of Animal Science and Veterinary Medicine, Heilongjiang Bayi Agricultural University, Daqing, Heilongjiang Province, 163319, China. [2]Branch of Animal Husbandry and Veterinary of Heilongjiang Academy of Agricultural Sciences, Qiqihar, Heilongjiang Province, 161005, China. [3]Department of Animal and Poultry Sciences, Virginia Polytechnic Institute and State University, Blacksburg, Virginia, USA.

[4]These authors contributed equally to this work.

*Corresponding author. Email: lishize@byau.edu.cn (S.Z. Li)

**Corresponding author. Email: xubin@byau.edu.cn (B. Xu)

Abstract

Objective: O-GlcNAcylation, a nutrient sensing pathway involved in a myriad of cellular processes, it plays a key role in metabolism homeostasis. Cold stress disturbs cellular metabolic and energy homeostasis and is one of the causes of stress-induced illnesses. It is reported that O-GlcNAcylation has been shown to be upregulated during cold stress. Skeletal muscle and its residential mitochondria play an important role in maintaining the metabolic homeostasis of the whole body. Nevertheless, the mechanism of which O-GlcNAcylation adapts to cold stress in skeletal muscle remains unknown.

Methods: To characterize the effect of O-GlcNAcylation on mouse skeletal muscle during cold exposure, this research investigated the effects of skeletal muscle structure, function, mitochondrial homeostasis, the deacetylation activity of SIRT1, acetylation expression levels and oxidative stress levels in *O*gt mKO mice by cold exposure (4 ℃, 3 h a day, for 1 week). In order to understand the mechanism of O-GlcNAcylation on skeletal muscle homeostasis under cold stress, C2C12 cells was used as a model *in vitro*. C2C12 cells were treated with OGT inhibitor (Alloxan) and OGA inhibitor (Thiamet G) to decrease and enhance O-GlcNAcylation signals in mild hypothermia, respectively, and then recapitulated *in vivo* phenotype. Finally, the interaction between OGT and SIRT1 was demonstrated, and the O-GlcNAcylation of SIRT1 played an important role in the imbalance of skeletal muscle homeostasis induced by cold exposure.

Results: Results showed that in addition to enhance cold stress-induced mitochondrial

abnormalities, cell senescence, and collagen accumulation, *Ogt* deficiency was found to induce autophagy, mitophagy and oxidative stress level in skeletal muscle during cold exposure. And the results showed that the expression level of SIRT1 was reduced, concomitant with increased expression and acetylation of FoxO1 in wild type mice challenged with cold stress. Because the depletion of *Ogt* further reduced SIRT1, and increased FoxO1 in muscle challenged with cold stress. Furthermore, this study showed that OGT had a physiological interaction with SIRT1. Thr^{160} and Ser^{161} sites of SIRT1 could be O-GlcNAcylation, and overexpression of SIRT1 saved mitochondrial defects in C2C12 cells caused by cold exposure.

Conclusion: Cold stress can cause skeletal muscle damage, and O-GlcNAcylation of SIRT1 is an important protection mechanisms of skeletal muscle's adaptation to cold stress.

Keywords: Cold stress; Skeletal muscle; Metabolic homeostasis imbalance; SIRT1; O-GlcNAcylation

1. Introduction

Energy metabolism is the basic characteristic of life, and any living body needs to maintain its own activities through metabolism. Skeletal muscle was the largest repository of protein in the body, and skeletal muscle energy metabolism plays an important role in maintaining the homeostasis of the body. The growth of skeletal muscle is a strict and complex molecularly regulated process, which has important connections with many signal transduction pathways, regulatory factors, and genes[1]. The damage of skeletal muscle homeostasis is closely related to many diseases[2], skeletal muscle diseases are associated with significant changes in metabolic pathways[3]. As an energy converter, mitochondria participate in aerobic respiration and produce ATP to supply energy for the body, which through mitochondrial fusion and fission, and mitochondrial biogenesis and mitophagy to regulation mitochondrial homeostasis in response to stress[4–6]. Research has shown that skeletal muscle health is linked to the number of mitochondria in muscle fibers and the ability to breathe. The addition of mitochondrial biogenesis can contribute to muscle energy metabolism and cellular stress responses such as autophagy and apoptosis[7,8]. Mitochondria remove damaged mitochondria through mitophagy and play an important role in cellular homeostasis[9–11]. It was reported that excessive mitochondrial fusion can enhance mitophagy, which can reduced mitochondrial mass and ATP production[12]. During aging, Mfn2 expression decreases and aberrant mitochondria accumulate contributing to sarcopenia[13,14]. Together, these findings suggested that mitochondrial homeostasis of skeletal muscle plays an important role

in maintaining energy metabolism and muscle mass. Cold is one of the inevitable environmental stressors in the life process. Under low temperature conditions, the body will have a series of adaptive responses, such as increased food intake, increased activity, and increased metabolic rate to increase body heat production and maintain energy balance. The thermogenesis of skeletal muscle is an essential survival mechanism for warm-blooded animals, and mammals adapt to the body's stimulation of the cold environment through skeletal muscle tremors and thermogenesis. It has been reported that when the ambient temperature drops, skeletal muscle tremor produces heat was five times more than resting[15]. In addition, the use of muscle glycogen and glucose uptake also increased with muscle tremor intensity during cold exposure[16].

O-linked β-D-N-acetylglucosamine (O-GlcNAcylation) is a post-translational modification that is closely related to intracellular and whole-body metabolic and energy metabolism[17,18]. Two enzymes are involved in O-GlcNAcylation cycling: O-linked N-acetylglucosamine transferase (OGT) adds, whereas O-GlcNAcase (OGA) removes, the O-GlcNAcylation moiety, respectively[19,20]. O-GlcNAcylation, a dynamic nutrient and stress sensitive post-translational modification, occurs on myriad proteins in the cell nucleus, cytoplasm and mitochondria. O-GlcNAcylation serves as a nutrient sensor to regulate signaling, transcription, translation, cell division, metabolism, and stress sensitivity in all cells[21]. Since O-GlcNAcylation has been regarded as a nutrient sensing pathway, it is not surprising that many mitochondrial proteins are O-GlcNAcylated. For example, proteins in the electron transport chain

such as NDUFA9 of complex I, core 1, and core 2 of complex III, and subunit I of complex IV (COX I), and proteins in the TCA cycles such as succinyl-coasynthetase (SUCLA2) and oxoglutarate dehydrogenase complex (OGDC), are O-GlcNAcylated[22,23]. Mitochondrial protein O-GlcNAcylation has been shown to play an essential role in whole body glucose homeostasis during cold stress[24]. In addition, O-GlcNAc/Akt pathway has been reported to regulate glucose metabolism and reduces apoptosis in pig liver under acute cold stress[25]. In brown adipose tissue, O-GlcNAcylation plays a pivotal role in cold-induced thermogenesis mitochondrial biogenesis. Still, others reported that acute cold stress can increase O-GlcNAcylation levels in mice, accompanied by a reduction of apoptosis and autophagy[26]. Together, these findings suggested that O-GlcNAcylation may serve to promote cell survival and balance cellular metabolism during cold stress.

Acetylation is one of the major post-translational protein modifications in cells and which also was an important regulatory mechanism for autophagy[27]. The interplay between acetylation and deacetylation is critical for many important cellular processes, and when acetylation mechanisms are disturbed, such as histone acetylation, the body will develop serious disease[28,29]. Silent information regulator factor 2-related enzyme 1 (Sirtuin 1, SIRT1) is a NAD^+-dependent deacetylase involved in the regulation of a wide range of biological processes, including cell senescence, energy balance, and oxidative stress[30,31]. Since NAD^+/NADH are energy sources for the electron transport chain in mitochondria, and NAD^+ is the substrate of SIRT1, SIRT1 may play an important role in the regulation of mitochondrial oxidative

117 phosphorylation. In addition, SIRT1 activation has been reported to cause the demise
118 or turnover of damaged mitochondria potentially through mitophagy[32–35]. In this
119 sense, SIRT1 has an important role in the maintenance of mitochondrial health[36].
120 Furthermore, SIRT1 has been established as a critical regulator of general
121 macroautophagy and is broadly viewed as one of the cellular protective mechanisms
122 against stress and death insults[37–39]. Upstream, it has been reported that the
123 O-GlcNAcylation of SIRT1 is elevated during genotoxic, oxidative, and metabolic
124 stresses; SIRT1 O-GlcNAcylation increases its deacetylase activity and protects cells
125 from stress-induced apoptosis[40]. Downstream, SIRT1 has a large number of targets,
126 one of which is Forkhead box class O family member proteins (FoxOs). SIRT1
127 regulates the activity of FoxOs, which in turn, modulate the activity of SIRT1[41].
128 FoxOs modulate numerous targets, such as genes involved in apoptosis and autophagy,
129 anti-oxidative enzymes, cell cycle arrest genes, and metabolic and immune
130 regulators[42,43]. FoxOs also regulate two main proteolytic systems, the
131 ubiquitin-proteasome, and the autophagy-lysosome systems, including mitophagy[44].
132 Given the multifaceted functions of FoxOs, it is reasonable to speculate that SIRT1's
133 modulation of FoxO activity could influence mitochondrial function via gene
134 expression in the nucleus and mitochondria-to-nucleus retrograde signaling. Together,
135 these findings suggested that SIRT1 and O-GlcNAcylation have certain effects on
136 maintaining cellular homeostasis under stressful conditions.
137 In conclusion, O-GlcNAcylation modification can play the role of "nutrition and
138 stress receptor" in the body's response to stress, and SIRT1 is essential for

maintaining mitochondrial homeostasis and apoptosis. So what roles do they play in skeletal muscle adaptation to cold exposure? In this study, the O-GlcNAcylation of SIRT1 was used as the target to explore the regulatory mechanism of skeletal muscle adaptation to cold exposure.

2. Materials and Methods

2.1. Mouse experiments

In all mouse experiments, 6-weeks-old male mice were used in the experiment. *Ogt*$^{LoxP/+}$ mice were purchased from the Jackson Laboratory (JaxMice, strain#: 004860, allele symbol: B6.129-*Ogt*^{tm1Gwh}/J). *Ogt* gene knockout was achieved by breeding *HSA*$^{Cre/+}$ (JaxMice, strain#: 006149, allele symbol: B6.Cg-Tg (ACTA1-cre) 79Jme/J) males with *Ogt*$^{LoxP/LoxP}$ females to generate *HSA*$^{+/+}$; *Ogt*$^{LoxP/Y}$ (WT) and *HSA*$^{Cre/+}$; *Ogt*$^{LoxP/Y}$(*Ogt* mKO) mice. Mice were fed in individually ventilated cages (IVC) at an ambient temperature of 26 ℃ ± 2 ℃ under a 12 h light/dark cycle with free access to food and water. For cold stress experiments, mice were exposed to 4 ℃ for 3 h a day for a period of one week. All animal procedures were approved and conducted in accordance with the guidelines set by Heilongjiang Bayi Agricultural University Animal Care and Use Committee.

2.2. Histological staining

Muscles were isolated and fixed with 10% formalin for 24 h, then make tissue sections. Masson trichrome staining was performed according to the manufacturer's instructions (Solarbio Life Sciences, G1346). β-Galactosidase staining kit was

purchased from the Beyotime Biotechnology (C0602) and the staining was performed according to the manufacturer's instruction. Images were taken using a fluorescent microscope (High resolution slide scanning system, Pannoramic MIDI, 3DHISTECH Ltd, Hungary).

2.3. Western blotting

Muscles tissues or C2C12 cells were lysed in ice-cold RIPA Lysis Buffer (Beyotime biotechnology, P0013B) containing 1% protease and PMSF (Beyotime biotechnology, ST506) on ice. After collection of lysate removed debris by centrifugation, protein concentrations were measured by BCA assay (Beyotime biotechnology, P0010S). Mitochondrial extract and nuclear extract from muscles tissues or C2C12 cells using Mitochondria Isolation Kit (Beyotime Biotechnology, C3606) and Nuclear and Cytoplasmic Protein Extraction Kit (Beyotime Biotechnology, P0028). Protein samples were mixed with SDS-PAGE Sample Loading Buffer (Beyotime Biotechnology, P0015) and incubated at 70 °C for 10 min. Proteins were transferred to 0.45 μm PVDF membranes (Merck Millipore, IPVH0010), and blocked with 5% skim milk in 10 mM Tris TBS-0.1% Tween 20 (TBST) for at least 1 h. Primary and HRP conjugated secondary antibodies (Table S1) were diluted in 5% skim milk in TBST. HRP substrate ECL (Merck Millipore, WBKLS0500) were used to detect signals. Band intensities were quantified by Image-Pro Plus. The antibodies used for western blotting analysis were as follows: MGEA5/OGA antibody (Abcam, ab124807); OGT/*O*-Linked N-Acetylglucosamine Transferase (Abcam, ab96718); O-GlcNAc antibody (CTD110.6, CST, 9875); SIRT1 polyclonal antibody (Proteintech, 1:1000, 13161-1-AP); FoxO1 polyclonal antibody (Proteintech, 1:1000, 18592-1-AP); AC-FoxO1 (Abclonal, 1:1000, 3560748323); Acetylated-lysine antibody (CST,

1:1000, 9441); P62/SQSTM1 polyclonal antibody (Proteintech, 1:1000, 18420-1-AP); Beclin1 polyclonal antibody (Proteintech, 1:1000, 11306-1-AP); ATG5 polyclonal antibody (Proteintech, 1:1000, 10181-2-AP); LC3 polyclonal antibody (Proteintech, 1:1000, 14600-1-AP); DRP1 (C-terminal) polyclonal antibody (Proteintech, 1:1000, 12957-1-AP); MFN1 polyclonal antibody (Proteintech, 1:1000, 13798-1-AP); PINK1 polyclonal antibody (Proteintech, 1:1000, 23274-1-AP); PARK2/Parkin polyclonal antibody (Proteintech, 1:1000, 14060-1-AP); Nrf2 rabbit polyclonal antibody (ABclonal, 1:1000, A1244); Histone-H3 polyclonal antibody (Proteintech, 1:1000, 17168-1-AP); Acetyl-Histone H3 (Lys9) (C5B11) rabbit monoclonal antibod (CST, 1:1000, 9649); VDAC polyclonal antibody (Proteintech, 1:1000, 10866-1-AP); Lmin B1 polyclonal antibody (Proteintech, 1:2000, 12987-1-AP); alpha tubulin monoclonal antibody (Proteintech, 1:20000, 66031-1-Ig); HRP-conjugated Affinipure Goat Anti-Mouse IgG (H+L) (Proteintech, 1:10000, SA00001-1); HRP-conjugated affinipure goat anti-rabbit IgG (H+L) (Proteintech, 1:10000, A00001-2).

2.4. Reactive oxygen species (ROS) detection

Mouse skeletal muscle were quickly frozen, cut to a thickness of 8 μm, and placed on glass slides. Fresh dihydroethidium (DHE) solution (Beyotime Biotechnology, S0063) was applied to each tissue section, and the section was incubated for 30 min at 37 ℃ in the dark. Fluorescent images were captured using a fluorescent microscope (High resolution slide scanning system, Pannoramic MIDI, 3DHISTECH Ltd, Hungary). ROS detection in C2C12 cells, After mild hypothermia treatment (32 ℃), C2C12 cells stained using a ROS assay kit following the manufacturer's instructions (Beyotime, Reactive Oxygen Species Assay Kit, S0033S). The cells were then analyzed using a flow cytometer (Beckman, CytoFLEX FCM, USA).

2.5. MDA assay

Muscles tissues or C2C12 cells were lysed in ice-cold RIPA Lysis Buffer (Beyotime biotechnology, P0013B) containing 1% protease and PMSF (Beyotime biotechnology, ST506) on ice. After collection of lysate removed debris by centrifugation, protein concentrations were measured by BCA assay (Beyotime biotechnology, P0010S). Protein concentration was determined using Enhanced BCA Protein Assay Kit (Beyotime, P0010S). The Lipid Peroxidation MDA Assay Kit (Beyotime, S0131) was used to measure lipid peroxidation at 532 nm using a microplate reader (Mindray, MR-96A, China).

2.6. Cell mitochondrial stress test

Fresh muscle tissue was washed in DMEM, cut, and placed in the islet capture plate. C2C12 cells were seeded into XF cell culture microplates. Before the experiments, the probe plate containing XF calibrant was cultured overnight in a carbon dioxide-free incubator to achieve balance. During the experiment, the medium was changed to XF test medium supplemented with 5 mM sodium pyruvate, 10 mM glucose and 2 mM glutamine, and balanced in a non-CO_2 incubator for 1 h. Oxygen consumption rate (OCR) were monitored by sequential injections of 1.5 μM oligomycin, 1μM FCCP and 0.5 μM rotenone/antimycin A (Seahorse XF Cell Mito Stress Test Kit, Agilent, Santa Clara, CA) according to the manufacturer's instructions.

2.7. NAD^+ measurement

Fresh muscle tissue or C2C12 cells was collected and rinsed with ice-cold PBS. NAD^+ and NADH levels of muscle tissue and C2C12 cells were measured at 450 nm

with a microplate analyzer using the NAD^+/NADH Assay Kit with WST-8 (Beyotime, S0175). The following formula was used to derive NAD^+: $NAD^+ = NAD_{total} – NADH$.

2.8. Determination of SIRT1 activity

Fresh muscle tissue or C2C12 cells was collected, rinsed with ice-cold PBS, and extract nuclear protein using nuclear and cytoplasmic protein extraction kit (Beyotime, P0027). SIRT1 activity was measured using a commercial kit following the manufacture's instruction (Sigma, CS1040). Fluorescence intensity was detected by fluorescence microplate reader, and the activity of SIRT1 was calculated. Excitation = 340 – 380 nm, Emission = 430 – 460 nm.

2.9. Detection of glycosylation

Muscle tissue or C2C12 cells were lysed using the NP-40 Lysis Buffer (Beyotime, P0013F). Protein concentration was determined using the Enhanced BCA Protein Assay Kit (Beyotime, P0010S). 30 μL of agarose succinylated wheat germ agglutinin (Vectorlabs, AL-1023S) was added to 500 μg total lysate. The mixture was then incubated overnight at 4 ℃, centrifuged for 2 min at 3,500 rpm the next day, and the supernatant was discarded. The beads were then washed 3 times with NP-40 Lysis Buffer (Beyotime, P0013F) and the supernatant was discarded. SDS-PAGE Sample Loading Buffer (Beyotime, P0015L) was added to the beads and was boiled for 5 min. The supernatant was collected and used for western blotting analysis.

2.10. Mitochondrial imaging

When C2C12 cells reached 70% confluence, culture medium was removed and the

working solution of MitoTracker Red CMXRos (Beyotime, C1049) was added to the cells. After an incubation at 37 ℃ for 30 min, the medium was changed to fresh culture medium pre-warmed at 37 ℃. Images were taken using a laser scanning confocal microscope (Leica, TCS-SP2, Germany).

2.11. Imaging of mitochondrial membrane potential using JC-1

When C2C12 cells reached 70% confluence, medium was removed and cells were washed once with PBS. 1 mL of the working fluid JC-1 (Beyotime, C2006) was added to the cells according to the manufacturer's instructions. Images were taken using a laser scanning confocal microscope (Leica, TCS-SP2, Germany).

2.12. Immunofluorescence

C2C12 cells were fixed with 4% paraformaldehyde, permeabilized with 0.3% Triton X-100, and blocked with 3% bovine serum albumin. Cells were then incubated in the primary antibody solutions overnight at 4 ℃. After incubation in the primary antibody overnight at 4 °C, sections were washed in 1 × PBS three times with 5 min each. The cell crawing were then incubated in Alexa Fluor coraLite488-conjugated Affinipure Goat Anti-Mouse IgG (Proteintech, SA00013-1) or Alexa Fluor coraLite594-conjugated Goat Anti-Rabbit IgG (Proteintech, SA00013-4) highly cross-absorbed antibodies, respectively, for 1 h at room temperature, washed in PBS, and mounted in fluorescent mounting medium for microscopy. Images were taken using a laser scanning confocal microscope (Leica, TCS-SP2, Germany).

2.13. Statistical analysis

All statistical parameters were calculated using Graphpad Prism 8.0.1 software (Graphpad Software, San Diego, CA, USA). Values were expressed as means ± standard deviation (SD). Statistical comparisons were assessed across different treatment groups (room temperature and cold exposure) and different type mice groups (wild type and *Ogt* mKO mice). All data analyses of the wild type and *Ogt* mKO mice groups were performed using two-way ANOVA *in vivo*. *In vitro*, statistical comparisons were assessed across different treatment groups. All data analyses were performed using one-way ANOVA and student's t-test. $P < 0.05$ was considered statistically significant.

3. Results

3.1. *Ogt* mKO accelerated skeletal muscle damage caused by cold exposure

Since O-GlcNAcylation plays an important role in modulating cellular metabolic homeostasis[45–47], OGT was specifically ablated in skeletal muscle using a human skeletal muscle α-actin-driven Cre/LoxP system. The knockouts of OGT and O-GlcNAcylation were confirmed using anti-OGT and O-GlcNAc antibodies (Figure 1A). In response to cold stress, OGT and O-GlcNAcylation-modified proteins were significantly up-regulated (Fig. 1A). Cold stress can affect a wide range of biochemical processes in mammals, particularly metabolism, and skeletal muscle is a major metabolic tissue in mammals. To study the effects of cold exposure on skeletal muscle aging and fibrosis, muscle sections were stained for markers. Both fibrosis

(Figure 1B) and aging markers (Figure 1C) of skeletal muscle were increased in response to cold stress, *Ogt* deficiency accelerated fibrosis and aging of skeletal muscle during cold exposure. In addition, the results showed that the mitochondrial morphology was abnormal after cold exposure, and which was more serious in *Ogt* mKO mouse (Figure. 1D). In brief, these data indicated that cold exposure can cause damage to the structure of skeletal muscle and its organelles, especially mitochondria, and *Ogt* deficiency appeared to exacerbate cold stress syndrome.

3.2. OGT deficiency exacerbate autophagy and oxidative stress during cold exposure

Autophagy is a cytoprotective mechanism that maintains cellular homeostasis by specifically degrading damaged or redundant organelles. However, excessive autophagy can be detrimental[48,49]. In our previous study, cold stress can promote autophagy in mouse liver[26]. This research assessed whether cold exposure had any effects on autophagy in skeletal muscle. Protein abundance of autophagy markers including P62/SQSTM1, Beclin1, ATG5, and LC3B were upregulated by cold stress, and their levels were further increased when OGT was ablated (Figure 2A). Since mitochondria was found deformed in response to cold stress (Fig. 1D), then whether mitophagy was also increased in skeletal muscle. Mitophagy markers PINK1 andubiquitin ligase Parkin, two enzymes involved in degrading the damaged mitochondria[50], were increased in cold stressed muscle, and even further increased in cold-stressed *Ogt* mKO muscle (Figure 2B). Since fission and fusion are important

for mitochondrial growth, redistribution, and mitochondrial network maintenance, this research measured the protein abundance of mitochondrial fission marker DRP1 and fusion marker MFN1, and found that these two markers followed the same pattern as PINK1 and Parkin (Fig. 2B). Since accumulation of ROS can lead to oxidative stress and mitochondrial dysfunction, which in turn, may result in organelle autophagy and cell apoptosis[51]. Meanwhile, this research measured oxidative stress and apoptosis-related markers in muscle. Results showed that the content of ROS and malondialdehyde (MDA), end-products of peroxidation of polyunsaturated fatty, increased dramatically in response to cold stress, particularly in the *Ogt* mKO muscle (Figure 2C, D). Then the research tested mitochondrial function by cell mitochondria stress test. Results showed that mitochondrial basal respiration, ATP production, maximal respiration, and spare respiratory capacity were significantly downregulated in cold-stressed muscle, and lack of OGT further compromised mitochondrial functions (Figure 2E). Together, these data suggested that cold stress may induce autophagy, mitophagy, oxidative stress and ROS-associated mitochondrial damages.

3.3. Cold stress enhanced protein acetylation in muscle through SIRT1 inhibition

Since acetylation and deacetylation have been shown to be involved in autophagy initiation and selective autophagy[52], this research measured the abundance of the acetylated proteins in muscle. The results showed that acetylated proteins in muscle were significantly upregulated in response to cold stress, particularly in *Ogt* mKO mice (Figure 3A). Since SIRT1 can deacetylate histone and histone modifying

enzymes[53], this research quantified the abundance of SIRT1 and histone H3 acetylated at lysine 9. The results showed that SIRT1 was significantly downregulated whereas H3 acetylation at lysine 9 was upregulated (Fig. 3A). Since both oxidative stress and acetylation have been shown to regulate FoxO1 activity[54], the research measured FoxO1 abundance and FoxO1 lysine acetylation at sites 262, 265, and 274, which were upregulated by cold (Fig. 3A). Furthermore, SIRT1 substrates NAD^+, SIRT1 deacetylase activity, and SIRT1 mRNA level were all significantly decreased (Figure 3B–D). Together, these data suggested that cold stress may increase acetylation of muscle proteins through downregulation of SIRT1, and then activated autophagy and mitophagy.

3.4. Mild hypothermia treatment in C2C12 cells recapitulated *in vivo* phenotype

Hypothermia is an involuntary drop in body temperature below 35 ℃. Depending on severity, low temperature can be classified as mild hypothermia (32 to 35 ℃), moderate hypothermia (28 to 32 ℃), severe hypothermia (under 28 ℃), and profound hypothermia (less than 24 ℃)[55]. Given that moderate and severe hypothermia may affect cell growth and survival, C2C12 cells were treated at mild hypothermia (32 ℃) for different periods (3 h, 6 h, and 9 h). The results showed that mild hypothermia induced autophagy and mitophagy, and upregulated O-GlcNAcylation in C2C12 cells, similar to *in vivo* mouse cold stress syndrome (Supplementary Figure 1A, B). Therefore, this research chose 3 h as the mild hypothermia treatment in the following experiments.

3.5. Inhibition of O-GlcNAcylation induced excessive autophagy and mitophagy in C2C12 cells under mild hypothermia

To gain a mechanistic insight of O-GlcNAcylation under cold stress, C2C12 cells was used as a model *in vitro*, and were treated with mild hypothermia with OGT inhibitor (Alloxan) and OGA inhibitor (Thiamet G) to decrease and enhance O-GlcNAcylation signals, respectively. Since oxidative stress can induce premature aging of cell and SA-β-gal is a biomarker [56,57], activity of SA-β-gal was measured. The results showed that mild hypothermia led to accumulation of SA-β-gal, which was consistent with *in vivo* mouse model (Figure 4A). Inhibition of OGT enhanced, whereas inhibition of OGA ameliorated, cold-induced aging (Fig. 4A). The Results showed that C2C12 cells mitochondria were disorganized after cold exposure (Figure 4B). This research also examined autophagy and mitophagy markers under mild hypothermia and mild hypothermia enhanced these markers. Inhibition of OGT worsened, whereas inhibition of OGA rescued, these defects (Figure 4C–D). Together, these data suggested that O-GlcNAcylation protects cells from cold-induced cell stresses.

3.6. Mild hypothermia caused imbalance of mitochondrial homeostasis in C2C12 cells

To study the effect of mild hypothermia on mitochondria in C2C12 cells, this research used MitoTracker Red CMXRos to detect mitochondrial abundance and C2C12 cells mitochondria reduced in number in response to cold stress; inhibition of OGT by

392 Alloxan worsened, but inhibition of OGA by TMG rescued, this defect (Figure 5A).
393 JC-1 is fluorescence probe widely used as a sensitive marker to detect mitochondrial
394 membrane potential (ΔΨm)[58]. When mitochondrial membrane potential is high,
395 JC-1 aggregated in the mitochondria matrix and formed J-aggregates, producing red
396 fluorescence. The results showed that mitochondrial membrane potential of C2C12
397 cells decreased under mild hypothermia. Inhibition of OGT further lowered
398 mitochondrial membrane potential, whereas inhibition of OGA rescued the defect
399 (Figure 5B). Moreover, mild hypothermia significantly downregulated the basal
400 respiration, ATP production, maximum respiration, and spare respiratory capacity of
401 the isolated mitochondria. Inhibition of OGT further damaged mitochondrial function,
402 whereas inhibition of OGA rescued the defect (Figure 5C). Since nuclear factor
403 E2-related factor 2 (Nrf2) has been shown to regulate antioxidant defense to protect
404 cells from oxidative stress[59], the cells were stained with anti-Nrf2 antibody. The
405 results showed that mild hypothermia induced Nrf2 expression. Inhibition of OGT
406 enhanced Nrf2 expression whereas inhibition of OGA reversed it (Figure 5D). To
407 detect ROS production, C2C12 cells were loaded with Dichlorodihydrofluorescein
408 diacetate (DCFH-DA), a well-known probe for the detection of intracellular hydrogen
409 peroxide (H_2O_2) as well as oxidative stress[60]. Flow cytometric data showed that
410 mild hypothermia enhanced ROS production; inhibition of OGT further increased,
411 whereas inhibition of OGA rescued, this defect (Figure 5E). MDA is a final product of
412 polyunsaturated fatty acid peroxidation and thus a marker of oxidative stress[61]. The
413 results showed that mild hypothermia induced MDA overproduce. Inhibition of OGT

414 enhanced MDA production whereas inhibition of OGA reversed this process (Figure
415 5F).
416
417 **3.7. Mild hypothermia inhibited SIRT1 O-GlcNAcylation in C2C12 cells**
418 To address whether cold stress regulates SIRT1 in the same way in C2C12 cells as *in*
419 *vivo*, this research measured NAD^+, SIRT1 deacetylase activity, and Sirt1 transcript.
420 Consistent with the *in vivo* data, all three measures were decreased by cold stress,
421 further reduced by OGT inhibitor but rescued by OGA inhibitor (Figure 6A–C).
422 Accordingly, the acetylated proteins including FoxO1 in C2C12 cells was
423 significantly increased (Figure 6D). Since SIRT1 is responsive to O-GlcNAcylation
424 under cold stress, SIRT1 should have physical interaction with OGT was predicted.
425 This finding was further confirmed using succinylated wheat germ agglutinin (sWGA)
426 (Figure 6E). This research then used YinOYang 1.2 to predict the O-GlcNAcylation
427 sites of SIRT1, and results showed that the Thr^{160} and Ser^{161} on SIRT1 were putative
428 O-GlcNAcylation sites, consistent with a recent report[62]. This research then aligned
429 the amino sequences across species and found that Ser 161 site was conserved across
430 species. Together, these findings suggested that OGT can physically modified SIRT1.
431
432 **3.8. Overexpression of SIRT1 rescued mitochondrial defects in C2C12 cells**
433 **under mild hypothermia**
434 To test whether SIRT1 is the downstream effector that relays OGT action under cold
435 stress, this research generated SIRT1 wild-type and double-site mutants

(Thr^{160}/Ser^{161}→Ala, named SIRT1-E2^{mut-AA}). This research then transfected wild-type and the mutant plasmids into C2C12 cells to assess whether SIRT1 overexpression can rescue cold stress effects. These data showed that wild-type SIRT1 overexpression could reduce the autophagy and mitophagy, whereas the mutant SIRT1 failed to do so (Figure 7A, B). The results showed that wild-type SIRT1 overexpression could reduce Nrf2 expression (Figure 7C, D), reduce ROS and MDA produce (Figure 7E, F). The research then used MitoTracker Red CMXRos to detect mitochondrial abundance and C2C12 cells mitochondria increase in number in response to wild-type, but not mutant, SIRT1 overexpression (Figure 8A). Wild-type SIRT1 overexpression could improve the mitochondrial membrane potential of C2C12 cells, whereas the mutant SIRT failed to do so (Figure 8B). Basal respiration, ATP production, maximum respiration, and spare respiratory capacity of C2C12 cells have been improved by overexpressing wild-type, but not mutant, SIRT1 (Figure 8C). Together, these data suggested that SIRT1 conveys, at least in part, OGT action in C2C12 cells's response to mild hypothermia.

4. Discussion

These data suggested that cold stress can induce mitochondrial homeostasis imbalance, which led to skeletal muscle damage. O-GlcNAcylation of SIRT1 at the Thr^{160} and Ser^{161} sites contributed to the adaptation of skeletal muscle to cold exposure.

Cold stress affects a variety of biochemical regulatory systems and has a major impact on thermogenesis, immune responses, and metabolism. However, the effect of cold

458 stress on skeletal muscle metabolism is not clear. Although it is not surprising that
459 pathways involved in autophagy, mitophagy in particular, are upregulated by cold
460 stress, it is interesting to know the pathways responsible for mitochondrial fission and
461 fusion are also upregulated. This upregulation may suggest a compensatory
462 mechanism for the muscle to meet the energy demand depleted by the damaged
463 mitochondria population.
464 O-linked N-acetylglucosamine (O-GlcNAc) transferase (OGT) is a unique enzyme
465 introducing O-GlcNAc moiety on target proteins, and it critically regulates various
466 cellular processes in diverse cell types. It has been reported that OGT is involved in
467 several processes, including circadian regulation of gene expression, positive
468 regulation of cold-induced thermogenesis and regulation of gluconeogenesis. Cold
469 stress or β-adrenergic stimulation activates PERK that phosphorylates OGT, which in
470 turn glycosylates TOM70 on Ser94, enhancing MIC19 protein import into
471 mitochondria and promoting cristae formation and respiration[63]. It has also been
472 reported that OGT regulates hematopoietic stem cell maintenance via
473 PINK1-Dependent mitophagy[64]. Therefore, the finding of OGT in mitochondrial
474 function and mitophagy under cold stress is not new. Of note, OGT as a nutrient
475 sensor, together with its cycling partner OGA, was also upregulated by cold stress.
476 Considering the sensory role that OGT plays in modulating cellular activities to match
477 the level of nutrient availability, we hypothesized that enhanced OGT expression and
478 the ensuing O-GlcNAcylation of its substrates serve as a protective mechanism for
479 muscles to mobilize the metabolic and energy resources to fight against cold stress.

Evidences from this study supported this hypothesis in that OGT knockout exacerbated the cold stress syndrome in skeletal muscle. In muscle, as in other metabolically active tissues such as liver and adipose tissue, OGT has thousands of substrates that are “awaiting messages” (via O-GlcNAcylation) from the nutrient sensor OGT to change their functions and/or localization. Although the exact mechanism of how OGT and its thousands of substrates interact to help cells adapt to cold stress, it is clear that OGT plays an instrumental rather than detrimental role in this pathological process. To further support this argument, inhibiting OGA activity by a specific inhibitor TMG ameliorates the cold stress syndrome in skeletal muscle.

From mechanistic standpoint, this research proposed that OGT functions through its substrate SIRT1 to regulate the cellular responses to cold stress. There are three lines of evidence to support this thesis: First, SIRT1’s expression and activity are downregulated during cold stress both *in vivo* and *in vitro*; correspondingly, the cellular acetylation level dramatically increases. SIRT1 is an NAD^+ dependent deacetylase that plays a key role in a wide range of biological events, including metabolism, immune response, and aging[65]. In this study, the results showed that FoxO1 protein expression and acetylation were increased under cold stress, accompanied by down-regulation of SIRT1 expression and activity. Since FoxO1 is involved in autophagy and mitophagy[66,67], it is reasonable to speculate that muscle responds to cold stress by increasing the expression of OGT, which glycosylates and thus stabilizes SIRT1. O-GlcNAcylated SIRT1 then deacetylates and downregulates the effect of FoxO1 on autophagy/mitophagy. This argument was supported by the

fact that under mild hypothermia inhibition of OGA led to decreases in FoxO1 expression and FoxO1 acetylation, where inhibition of OGT had opposite effect. Since SIRT1 can deacetylate a broad range of substrates ranging from histone families such as $H1^{K26}$, $H3^{K9}$, and $H4^{K16}$, DNA damage repair-related proteins such as NBS1 and Ku70, gluconeogenesis factors such as CRTC2, and immune response factors such as NF-κB and FOXP3[68], it was difficult to pinpoint which substrated or substrated combinations are responsible for the observed actions of SIRT1 on autophagy/mitophagy under cold stress. For example, in addition to working through FoxO1, SIRT1 had been reported to regulate autophagy and mitophagy through PGC1 and Mfn2[69,70]. Regardless, this research speculated that FoxO1 replays, at least in part, SIRT1 actions in cold-induced autophagy and mitophagy. This research further proposed that OGT adds a sugar derivative to SIRT1 to either increase its stability or protect it from degradation. Since protein acetylation can occur on a myriad of proteins and such a modification can activate or silence the expression of a host of genes and change the activity and locations of multitude enzymes, one can imagine how important it is to finetune such a posttranslational modification. These results showed that cold stress can induce protein acetylation with a concomitant downregulation of SIRT1 expression. It is possible that downregulation of SIRT1, along with other deacetylases, were responsible for the enhanced acetylation during cold stress. Second, this study demonstrated the physical interaction of OGT and SIRT1 by enriching O-GlcNAcylation proteins using succinylated wheat germ agglutinin (sWGA) and detecting the expression of SIRT1 (Figure 6E). Third, it is

524 reported that the Thr^{160} and Ser^{161} sites of SIRT1 are O-GlcNAcylated[62]. Therefore,
525 this study further demonstrated the protective effect of SIRT1 O-GlcNAcylation at
526 Thr^{160} and Ser^{161} sites on skeletal muscle during cold stress.
527 Mitochondrial cells are the main place for aerobic respiration, which also are the
528 center of energy generation and material metabolism. When the homeostasis of the
529 intracellular environment is unbalanced, mitochondrial damage can release
530 apoptosis-related proteins and produce a series of reactions, resulting in apoptosis[71].
531 A large number of studies have shown that when cells are stimulated by external,
532 mitochondrial function-related indicators are significantly down-regulated, such as
533 basal respiration, ATP production, maximal respiration, and spare respiratory
534 capacity[72-74]. The results of this study showed that basal respiration, ATP
535 production, maximum respiration and spare respiration capacity of C2C12 cells were
536 significantly down-regulated after mild hypothermia treatment, which were consistent
537 with the above reported research results. However, after SIRT1 was overexpressed,
538 the above indicators showed a significant up-regulation trend, and the mitochondrial
539 function of SIRT1 was not improved after SIRT1 was deglycosylated at Thr^{160} and
540 Ser^{161} sites. Mitochondrial membrane potential is a key indicator of mitochondrial
541 health[75]. Mito-tracker Red CMXRos is a cell permeable derivative of X-Rosamine
542 (Chloromethyl-X-rosamine, CMXRos), which can specifically label bioactive
543 mitochondria in cells. Detection of mitochondrial membrane potential[76]. The results
544 of this study showed that the mitochondrial membrane potential of C2C12 cells was
545 significantly decreased after mild hypothermia treatment; and after SIRT1 was

546 overexpressed, the membrane potential of C2C12 cells was significantly upregulated
547 after mild hypothermia treatment. However, the membrane potential of SIRT1 was not
548 restored after deletion of O-GlcNAcylation at Thr^{160} and Ser^{161} sites. The same
549 experimental results were obtained using JC-1 to detect mitochondrial membrane
550 potential. The above results all indicated that the mitochondrial function cells was
551 damaged after mild hypothermia treatment. ROS is an intermediate product of
552 mitochondrial aerobic respiration, and a small amount of ROS exists in cells under
553 physiological conditions. However, when mitochondrial function is damaged, a large
554 amount of ROS will be induced, resulting in an imbalance in the homeostasis of the
555 intracellular environment[77]. It has been proved that the mitochondrial membrane
556 potential of C2C12 cells decreased significantly after mild hypothermia treatment,
557 and a large number of ROS entered the cytoplasm through mitochondria, and then
558 induced damage of other organelles due to oxidative stress. The results of
559 transmission electron microscopy also proved that mitochondrial ridges of C2C12
560 cells disappeared after mild hypothermia treatment, and the morphology and structure
561 of which mitochondria were also damaged. In addition, the detection of autophagy
562 and mitophagy proteins by western blotting indicated the occurrence of autophagy
563 and mitophagy. Overexpression of SIRT1 alleviated autophagy and mitophagy in
564 C2C12 cells after mild hypothermia treatment. However, deletion of
565 O-GlcNAcylation of SIRT1 at Thr^{160} and Ser^{161} sites does not improve mild
566 hypothermic induced autophagy and mitophagy, as well as ROS production. MDA is a
567 product of lipid oxidation and can be used as a biomarker of oxidative stress[78]. The

568 results showed that the detection results of MDA in C2C12 cells were consistent with
569 that of ROS. These results suggested that mild hypothermia induced massive ROS
570 production and accumulation of MDA, causing oxidative stress in cells. Nrf2 is an
571 important antioxidant stress transcription factor and an important regulatory center to
572 maintain the intracellular redox state. Under normal conditions, Nrf2 locates in the
573 cytoplasm, but under the action of ROS, it enters the nucleus and activates the
574 transcriptional activity of downstream target genes, thereby enhancing antioxidant
575 activity. The results of western blotting and immunofluorescence showed that the
576 protein expression level of Nrf2 in the nucleus of C2C12 cells were significantly
577 up-regulated after mild hypothermia treatment, and the acetylation level of the 9th
578 amino acid of histone H3 was also significantly up-regulated. However, deletion of
579 O-GlcNAcylation at Thr^{160} and Ser^{161} sites in SIRT1 did not significantly change the
580 above phenomenon. In conclusion, this study speculated that cold exposure induced a
581 large accumulation of ROS and MDA in mouse skeletal muscle cells, resulting in
582 oxidative stress and a large amount of Nrf2 entering the nucleus, thereby improving
583 their antioxidant capacity. A large number of ROS can disrupt the structure and
584 function of mitochondria, resulting in an imbalance of intracellular environmental
585 homeostasis. However, the enhancement of SIRT1's O-GlcNAcylation signal at Thr^{160}
586 and Ser^{161} sites blocked this damage process. Autophagy is a cytoprotective
587 mechanism that maintains cellular homeostasis by specifically degrading damaged or
588 redundant organelles[79,80]. When homeostasis is unbalanced, autophagy cleans up
589 damaged cells by means of clearance and degradation, thus maintaining homeostasis,

590 and mitochondria are important organelles for the occurrence of autophagy. The
591 up-regulation of LC3B expression is a marker of autophagy, and Beclin1, as a key
592 protein of autophagy initiation and an important ubiquitin junction protein P62 in
593 autophagy degradation, plays an important role in autophagy. The results showed that
594 the expression levels of autophagy-related proteins in cells were significantly
595 up-regulated after cold exposure, indicating that cold exposure activated the overall
596 process of autophagy. However, enhanced O-GlcNAcylation signals at Thr^{160} and
597 Ser^{161} sites of SIRT1 slowed down autophagy. The results of transmission electron
598 microscopy also demonstrated the occurrence of autophagy induced by cold exposure,
599 and mitochondrial structure and morphology were abnormal. PINK1 is a Ser/Thr
600 kinase, which can enter the mitochondrial membrane and be degraded. When
601 mitochondria are damaged, the mitochondrial membrane potential decreases, at this
602 time, the mitochondrial membrane's ability to degrade PINK1 decreases, and PINK1
603 will accumulate on the outer membrane of mitochondria, thus increasing the
604 recruitment of Parkin and facilitating ubiquitination and degradation of damaged
605 mitochondria. The results showed that the protein expression level of PINK1/Parkin
606 in C2C12 cells, a mitophagy-related marker, were significantly up-regulated after
607 mild hypothermia treatment. However, enhanced O-GlcNAcylation signal at Thr^{160}
608 and Ser^{161} sites of SIRT1 blocked the recruitment of Parkin by PINK1, thereby
609 slowing the occurrence of mitophagy.
610 In summary, the results of this study indicated that the expression of SIRT1 in
611 cold-exposed mice was inhibited and the deacetylation level was reduced. Meanwhile,

the SIRT1-Foxo1 pathway is activated, leading to increased histone acetylation and oxidative stress, and more Nrf2 was recruited into the nucleus, resulting in impaired mitochondrial structure, abnormal function, excessive autophagy and mitophagy in skeletal muscle of mice. Meanwhile, this study showed that O-GlcNAcylation of SIRT1 at Thr(160) and Ser(161) sites can alleviate the imbalance of mitochondrial homeostasis in mouse skeletal muscle induced by cold, which is a protective mechanism of the body. A graphical summary of the above mechanism was shown in Figure 9. In conclusion, the O-GlcNAcylation of SIRT1 contributes to muscle cell adaptation during cold stress, providing an important target for understanding the mechanisms of skeletal muscle adaptation to cold stress. Nonetheless, it is unclear how O-GlcNAcylation of SIRT1 protected muscle cells from the exact downstream molecular pathways of autophagy and mitophagy. Further studies on downstream pathway networks will help to identify molecular targets for cold stress management. Although this study highlighted the importance of O-GlcNAcylation of SIRT1 in muscle adaptation to cold stress, other mechanisms can not be ruled out. For example, many mitochondrial proteins in the TCA cycle and electron transport chain are O-GlcNAcylated, so it is conceivable that these proteins would be hyperglycosylated during cold stress. How these hyperglycosylated proteins function to maintain mitochondrial integrity warrants further investigation.

Declarations

Ethics approval and consent to participate

All experimental and research procedures were approved by and in accordance with relevant guidelines and regulations. All animal procedures were approved and conducted in accordance with the guidelines set by Heilongjiang Bayi Agricultural University Animal Care and Use Committee.We took adequate steps to ensure that animals did not suffer unnecessarily at any stage of an experiment.

Consent for publication

All authors agree to publish this paper.

Availability of data and materials

The datasets generated for this study are available on request from the corresponding author.

Competing interests

The authors declare that they have no competing interests.

Funding

This work was supported by the National Natural Science Foundation of China (project no. 31972637 and no.31772695), the Key Program of Natural Science Foundation of Heilongjiang Province, China (ZD2019C004), the Foundation for Young Scholars of Heilongjiang Province, China (YQ2021C027) and Heilongjiang Bayi Agricultural University for San Heng San Zong , China (ZRCQC202003).

Authors contributions

Yu Cao, Hao Shi and Ye Li developed the rationale of the study and wrote the

manuscript, which was commented on by all authors; Yu Cao designed and performed most of the experiments with additional experimental contributions of Jing-Jing Lu, Meng Zhang, Wan-Hui Zhou, Xiao-Shuang Li assist in completing the experiment. Shi-Ze Li and Bin Xu supervised the study.

Acknowledgements

Not applicable.

Supplementary material

Supplementary Figure 1.

REFERENCES

[1] Schiaffino, S., Sandri, M., Murgia, M., 2007. Activity-dependent signaling pathways controlling muscle diversity and plasticity. Physiology (Bethesda) 22:269–278.

[2] Isaac, A.R., Lima-Filho, R.A.S., Lourenco, M.V., 2021. How does the skeletal muscle communicate with the brain in health and disease? Neuropharmacology 197:108744.

[3] Ceco, E., Weinberg, S.E., Chandel, N.S., Sznajder, J.L., 2017. Metabolism and skeletal muscle homeostasis in lung disease. American Journal of Respiratory Cell and Molecular Biology 57(1):28–34.

[4] Meyer, J.N., Leuthner, T.C., Luz, A.L., 2017. Mitochondrial fusion, fission, and mitochondrial toxicity. Toxicology 391:42–53.

[5] Chan, D.C. 2006. Mitochondria: dynamic organelles in disease, aging, and development. Cell 125(7):1241–1252.

[6] Tilokano, L., Nagashima, S., Paupe, V., Prudent, j., 2018. Mitochondrial dynamics: overview of molecular mechanisms. Essays Biochem 62(3):341–360.

[7] Nunnari, J., Suomalainen, A., 2012. Mitochondria: in sickness and in health. Cell 148(6):1145–1159.

[8] Carter, H.N., Kim, Y., Erlich, A.T., Zarrin-Khat, D., Hood, D.A., 2018. Autophagy and mitophagy flux in young and aged skeletal muscle following chronic contractile activity. Comparative Study 596(16):3567–3584.

[9] Wu, N.N., Zhang, Y.M., Ren, J., 2019. Mitophagy, mitochondrial dynamics, and

686 homeostasis in cardiovascular aging. Oxidative Medicine and Cellular Longevity
687 2019:9825061.
688 [10] Dombi, E., Mortiboys, H., Poulton, J., 2018. Modulating mitophagy in
689 mitochondrial disease. Current medicinal chemistry 25(40):5597–5612.
690 [11] Praharaj, P.P., Naik, P.P., Panigrahi, D.P., Bhol, C.S., Mahapatra, K.K., Patra, S.,
691 et al., 2019. Intricate role of mitochondrial lipid in mitophagy and mitochondrial
692 apoptosis: its implication in cancer therapeutics. Cellular and Molecular Life Sciences
693 76(9):1641–1652.
694 [12] Yu, M.F., Nguyen, N.D., Huang, Y.Q., Lin, D., Fujimoto, T.N., Molkentine, J.M.,
695 et al., 2019. Mitochondrial fusion exploits a therapeutic vulnerability of pancreatic
696 cancer. JCI Insight 5(16):e126915.
697 [13] Sebastián, D., Sorianello, E., Segalés, J., Irazoki, A., Ruiz-Bonilla, V., Sala, D., et
698 al., 2016. Mfn2 deficiency links age-related sarcopenia and impaired autophagy to
699 activation of an adaptive mitophagy pathway. The EMBO Journal 35(15):1677–1693.
700 [14] Hood, D.A., Memme, J.M., Oliveira, A.N., Triolo, M., 2019. Maintenance of
701 skeletal muscle mitochondria in health, exercise, and aging. Annual Review of
702 Physiology 10:19–41.
703 [15] Eyolfson, D.A., Tikuisis, P., Xu, X., Weseen, G., Giesbrecht, G.G., 2001.
704 Measurement and prediction of peak shivering intensity in humans. European Journal
705 of Applied Physiology 84(1–2):100-106.
706 [16] Sellers, A.J., Pallubinsky, H., Rense, P., Bijnens, W., Weijer, T.V.D.,
707 Moonen-Kornips, E., et al., 2021. The effect of cold exposure with shivering on

708 glucose tolerance in healthy men. Journal of Applied Physiology 130(1):193-205.
709 [17] Hart, G.W., Slawson, C., Ramirez-Correa, G., Lagerlof, O., 2011. Cross talk
710 between O-GlcNAcylation and phosphorylation: roles in signaling, transcription, and
711 chronic disease. Annual Review of Biochemisty 80(1):825–858.
712 [18] Issad, T., Masson, E., Pagesy, P., 2010. O-GlcNAc modification, insulin signaling
713 and diabetic complications. Diabetes & Metabolism 36(6):423–435.
714 [19] Nie, H., Yi, W., 2019. O-GlcNAcylation, a sweet link to the pathology of
715 diseases. Journal of Zhejiang University SCIENCE B 20(5):437–448.
716 [20] Wang, X., Feng, Z.H., Wang, X.Q., Yang, L., Han, S.J., Cao, K., et al., 2016.
717 O-GlcNAcase deficiency suppresses skeletal myogenesis and insulin sensitivity in
718 mice through the modulation of mitochondrial homeostasis. Diabetologia
719 59(6):1287–1296.
720 [21] Banerjee, P.S., Lagerlöf, O., Hart, G.W., 2016. Roles of O-GlcNAc in chronic
721 diseases of aging. Molecular Aspects of Medicine 51:1–15.
722 [22] Hu, Y., Suarez, J., Fricovsky, E., Wang, H., Scott, B.T., Trauger, S.A., et al., 2009.
723 Increased Enzymatic O-GlcNAcylation of mitochondrial proteins impairs
724 mitochondrial function in cardiac myocytes exposed to high glucose. Journal of
725 Biological Chemistry 2(1):284.
726 [23] Adam, R.A., Schell, J.C., Ha, C.M., Pepin, M.E., Khalimonchuk, O., Schwertz,
727 H., et al., 2020. Maintaining myocardial glucose utilization in diabetic
728 cardiomyopathy accelerates mitochondrial dysfunction. Diabetes 69(10):2094–2111.
729 [24] Ohashi, N., Morino, K., Ida, S., Sekine, O., Lemecha, M., Kume, S., et al., 2017.

730 Pivotal role of O-GlcNAc modification in cold-induced thermogenesis by brown
731 adipose tissue through mitochondrial biogenesis. Diabetes 66(9):2351–2362.
732 [25] Liu, Y., Xu, B., Hu, Y.J., Liu, P., Lian, S., Lv, H.M., et al., 2021. O-GlcNAc / Akt
733 pathway regulates glucose metabolism and reduces apoptosis in liver of piglets with
734 acute cold stress. Cryobiology 100:125–132.
735 [26] Yao, R.Z., Yang, Y.Y., Lian, S., Shi, H.Z., Liu, P., Yang, H.M., et al., 2018.
736 Effects of acute cold stress on liver O-GlcNAcylation and glycometabolism in mice.
737 International Journal of Molecular Sciences 19(9):2815.
738 [27] Drazic, A., Myklebust, L.M., Ree, R., Arnesen, T., 2016. The world of protein
739 acetylation. Biochim Biophys Acta 1854(10):1372–1401.
740 [28] Myklebust, L.M., Damme, P.V., Støve, S.I., Dörfel, M.J., Abboud, A., Kalvik,
741 T.V., et al., 2015. Biochemical and cellular analysis of Ogden syndrome reveals
742 downstream Nt-acetylation defects. Human Molecular Genetics 24(7):1956–1976.
743 [29] Popp, B., Støve, S.I., Endele, S., Myklebust, L.M., Hoyer, J., Sticht, H., et al.,
744 2015. De novo missense mutations in the NAA10 gene cause severe non-syndromic
745 developmental delay in males and females. European Journal of Human Genetics
746 23(5):602–609.
747 [30] Cantó, C., Gerhart-Hines, Z., Feige, J.N., Lagouge, M., Noriega, M., Milne, J.C.,
748 et al., 2009. AMPK regulates energy expenditure by modulating NAD+ metabolism
749 and SIRT1 activity. Nature 458(7241):1056–1060.
750 [31] Meng, X.F., Tan, J., Li, M.M., Song, S.L., Miao, Y.Y., Zhang, Q., 2016. Sirt1:
751 Role under the condition of ischemia/hypoxia. Cellular and Molecular Neurobiology

752 37(1):1–12.

753 [32] Tang, B.L., 2016. Sirt1 and the Mitochondria. Molecules and Cells 39(2):87–95.

754 [33] Ding, M.G., Feng, N., Tang, D.S., Feng, J.H., Li, Z.Y., Jia, M., et al., 2018.
755 Melatonin prevents Drp1-mediated mitochondrial fission in diabetic hearts through
756 SIRT1-PGC1α pathway. Journal of Pineal Research 65(2):e12491.

757 [34] Iwabu, M., Yamauchi, T., Okada-Iwabu, M., Sato, K., Nakagawa, T., Funata, M.,
758 et al., 2010. Adiponectin and AdipoR1 regulate PGC-1alpha and mitochondria by
759 Ca(2+) and AMPK/SIRT1. Nature 464(7293):1313–1319.

760 [35] Yoshii, S.R., Mizushima, N., 2015. Autophagy machinery in the context of
761 mammalian mitophagy. Biochimica Biophysica Acta (BBA) 1853(10 pt
762 B):2797–2801.

763 [36] Anne, B., Sweeney, L.B., Sturgill, J.F., Chua, K.F., Greer, P.L., Lin, Y.X., et al.,
764 2004. Stress-dependent regulation of FoxO transcription factors by the SIRT1
765 deacetylase. Science 303(5666):2011–2015.

766 [37] Ng, F., Tang, B.L., 2013. Sirtuins' modulation of autophagy. Journal of Cellular
767 Physiology 228(12):2262–2270.

768 [38] Ou, X., Lee, M.R., Huang, X.X., Messina-Graham, S., Broxmeyer, H.E., et al.,
769 2014. SIRT1 positively regulates autophagy and mitochondria function in embryonic
770 stem cells under oxidative stress. Stem Cells 32(5):1183–1194.

771 [39] Suzuki, M., Bartlett, J.D., 2014. Sirtuin1 and autophagy protect cells from
772 fluoride-induced cell stress. Biochimica Biophysica Acta (BBA) 1842(2):245–255.

773 [40] Han, C.F., Gu, Y.C., Shan, H., Mi, W.Y., Sun, J.H., Shi, M.H., et al., 2014.

774 O-GlcNAcylation of SIRT1 enhances its deacetylase activity and promotes
775 cytoprotection under stress. Nature Communications 8(1):1491.
776 [41] Jalgaonkar, M.P., Parmar, U.M., Kulkarni, Y.A., Oza, M.J., 2021. SIRT1-FoxOs
777 activity regulates diabetic complications. Pharmacological Research 175:106014.
778 [42] Sin, T.K., Yung, B.Y., Siu, P.M., 2017. Modulation of SIRT1-Foxo1 signaling
779 axis by resveratrol: implications in skeletal muscle aging and insulin resistance.
780 Cellular Physiology and Biochemistry 35(2):541–552.
781 [43] Murtaza, G., Khan, A.K., Rashid, R., Muneer, S., Hasan S.M.F., Chen, J.X., 2017.
782 FoxO Transcriptional Factors and Long-Term Living. Oxidative Medicine and
783 Cellular Longevity 2017(124):349–354.
784 [44] Sanchez, A.M.J., Bernardi, H., Py, G., Candau, R.B., 2014. Autophagy is
785 essential to support skeletal muscle plasticity in response to endurance exercise.
786 Ameriacn Journal of Physiology-Regulatory Integrative Comparative Physiology
787 307(8):R956–969.
788 [45] Liu, Y., Yao, R.Z., Lian, S., Liu, P., Hu, Y.J., Shi, H.Z., et al., 2021.
789 O-GlcNAcylation: the “stress and nutrition receptor” in cell stress response. Cell
790 Stress & Chaperones 26(2):297–309.
791 [46] Lambert M., Claeyssen, C., Bastide, B., Cieniewski-Bernard, C., 2020.
792 O-GlcNAcylation as a regulator of the functional and structural properties of the
793 sarcomere in skeletal muscle: An update review. Acta Physiologica (Oxf)
794 228(1):e13301.
795 [47] Huang, P., Ho, S.R., Wang, K., Roessler, B.C., Zhang, F.X., Hu, Y., et al., 2011.

796 Muscle-specific overexpression of NCOATGK, splice variant of O-GlcNAcase,
797 induces skeletal muscle atrophy. American Journal of Physiology-Cell Physiology
798 300(3):C456–465.
799 [48] Yang, Z.F., Klionsky, D.J., 2010. Mammalian autophagy: core molecular
800 machinery and signaling regulation. Current Opinion in Cell Biology 22(2):124–131.
801 [49] Wirawan, E., Berghe, T.V., Lippens, S., Agostinis, P., Vandenabeele, P., 2012.
802 Autophagy: for better or for worse. Cell Research 22(1):43–61.
803 [50] Bingol, B., Sheng, M., 2016. Mechanisms of mitophagy: PINK1, Parkin, USP30
804 and beyond. Free Radical Biology and Medicine 100:210–222.
805 [51] Li, L.L., Tan, J., Miao, Y.Y., Lei, P., Zhang, Q., 2015. ROS and Autophagy:
806 Interactions and Molecular Regulatory Mechanisms. Cellular and Molecular
807 Neurobiology 35(5):615–621.
808 [52] Wang, R., Wang, G.H., 2019. Protein Modification and Autophagy Activation.
809 Advances in Experimental Medicine and Biology 1206:237–259.
810 [53] Vaquero, A., Scher, M.B., Lee, D.H., Sutton, A., Cheng, H.L., Alt, F.W., et al.,
811 2006. SirT2 is a histone deacetylase with preference for histone H4 Lys 16 during
812 mitosis. Genes & Development. 20(10):1256–1261.
813 [54] Xing, Y.Q., Li, A., Yang, Y., Li, X.X., Zhang, L.N., Guo, H.C., 2018. The
814 regulation of FoxO1 and its role in disease progression. Life Sciences 193:124–131.
815 [55] Duong, H., Patel, G., 2022. Hypothermia. Stat Pearls (Internet) 1(27).
816 [56] Wang, Z., Wei, D.D., Xiao, H.Y., 2013. Methods of cellular senescence induction
817 using oxidative stress. Biological Aging 1048:135–144.

818 [57] Kamal, N.S.M., Safuan, S., Shamsuddin, S., Foroozandeh, P., 2020. Aging of the
819 cells: Insight into cellular senescence and detection Methods. European Journal of
820 Cell Biology 99(6):151108.
821 [58] Sivandzade, F., Bhalerao, A., Cucullo, L., 2019. Analysis of the Mitochondrial
822 Membrane Potential Using the Cationic JC-1 Dye as a Sensitive Fluorescent Probe.
823 Bio Protocol 9(1):e3128.
824 [59] Sajadimajd, S., Khazaei, M., 2018. Oxidative Stress and Cancer: The Role of
825 Nrf2. Current Cancer Drug Targets. 18(6):538–557.
826 [60] Evgeniy, E., Kusmartsev, S., 2010. Identification of ROS using oxidized DCFDA
827 and flow-cytometry. Advanced Protocols in Oxidative Stress II 594:57–72.
828 [61] Gaweł, S., Wardas, M., Niedworok, E., Wardas, P., 2004. Malondialdehyde
829 (MDA) as a lipid peroxidation marker. Wiad Lek 57(9-10):453–455.
830 [62] Chattopadhyay, T., Maniyadath, B., Bagul, H.P., Chakraborty, A., Shukla, N.,
831 Budnar, S., et al., 2020. Spatiotemporal gating of SIRT1 functions by
832 O-GlcNAcylation is essential for liver metabolic switching and prevents
833 hyperglycemia. Proceedings of the National Academy of Sciences of the United States
834 of America 117(12):6890–6900.
835 [63] Latorre-Muro, P., O'Malley, K.E., Bennett, C.F., Perry, E.A., Balsa, E., Tavares,
836 C.D.J., et al., 2021. A cold-stress-inducible PERK/OGT axis controls TOM70-assisted
837 mitochondrial protein import and cristae formation. Cell Metabolism 33(3):598–614.
838 [64] Murakami, K., Kurotaki, D., Kawase, W., Soma, S., FFukuchi, Y., Kunimoto, H.,
839 et al., 2021. OGT regulates hematopoietic stem cell maintenance via

840 PINK1-dependent mitophagy. Cell Reports 34(1):108679.
841 [65] Xu, C.Y., Wang, L., Fozouni, P., Evjen, G., Chandra, V., Jiang, J., et al., 2020.
842 SIRT1 is downregulated by autophagy in senescence and ageing. Nature Cell Biology
843 22(10):1170–1179.
844 [66] Liu, H.Y., Han, J.M., Cao, S.Y., Hong, T., Zhuo, D., Shi, J., et al. 2009. Hepatic
845 autophagy is suppressed in the presence of insulin resistance and hyperinsulinemia:
846 inhibition of FoxO1-dependent expression of key autophagy genes by insulin. Journal
847 of Biological Chemistry 284(45):31484–31492.
848 [67] Li, W., Du, M.M., Wang, Q.Z., Ma, X.J., Wu, L., Guo, F., et al., 2017. FoxO1
849 Promotes Mitophagy in the Podocytes of Diabetic Male Mice via the PINK1/Parkin
850 Pathway. Endocrinology 158(7):2155–2167.
851 [68] Zhai, Z.C., Tang, M., Yang, Y., Lu, M., Zhu, W.G., Li, T.T., 2017. Identifying
852 Human SIRT1 Substrates by Integrating Heterogeneous Information from Various
853 Sources. Scientific Reports 7(1):4614.
854 [69] Nemoto, S., Fergusson, M.M., Finkel, T., 2005. SIRT1 functionally interacts with
855 the metabolic regulator and transcriptional coactivator PGC-1{alpha}. Journal of
856 Biological Chemistry 280(16):16456–16460.
857 [70] Yan, H.Z., Qiu, C.M., Sun, W.W., Gu, M.M., Xiao, F., Zou, J., 2018. Yap
858 regulates gastric cancer survival and migration via SIRT1/Mfn2/mitophagy. Oncology
859 Reports 39(4):1671–1681.
860 [71] Xie, L.L., Shi, F., Tan, Z.Q., Li, Y.S., Bode, A.M., Cao, Y., 2018. Mitochondrial
861 network structure homeostasis and cell death. Cancer Science 109(12):3686–3694.

862 [72] Yin, X.J., Hong, W., Tian, F.J., Li, X.C.,2021. Proteomic analysis of decidua in
863 patients with recurrent pregnancy loss (RPL) reveals mitochondrial oxidative stress
864 dysfunction. Clinical Proteomics 18(1):9.
865 [73] Böhm, A., Keuper, M., Meile, T., Zdichavsky, M., Fritsche, A., Häring, H.U., et
866 al., 2020. Increased mitochondrial respiration of adipocytes from metabolically
867 unhealthy obese compared to healthy obese individuals. Sci Reports 10(1):12407.
868 [74] Easton, Z.J.W., Delhaes, F., Mathers, K., Zhao, L., Vanderboor, C.M.G., Regnault,
869 T.R.H., 2021. Syncytialization and prolonged exposure to palmitate impacts BeWo
870 respiration. Reproduction 161(1):73–88.
871 [75] Sakamuru, S., Attene-Ramos, M.S., Xia, M.H., 2016. Mitochondrial Membrane
872 Potential Assay. Methods in Molecular Biology 1473:17–22.
873 [76] Pan, L.J., Nie, L.T., Yao, S., Bi, A., Ye, Y., Wu, Y.M., et al., 2020. Bufalin
874 exerts antitumor effects in neuroblastoma via the induction of reactive oxygen
875 species- mediated apoptosis by targeting the electron transport chain. International
876 Journal of Molecular and Cellular Medicine 46(6):2137–2149.
877 [77] Zorov, D.B., Juhaszova, M., Sollott, S.J., 2014. Mitochondrial reactive oxygen
878 species (ROS) and ROS-induced ROS release. Physiological Reviews 94(3):909–950.
879 [78] Tsikas, D., 2017. Assessment of lipid peroxidation by measuring
880 malondialdehyde (MDA) and relatives in biological samples: Analytical and
881 biological challenges. Analytical Biochemistry 524:13–30.
882 [79] Gaweł, S., Wardas, M., Niedworok, E., Wardas, P., 2004. Malondialdehyde
883 (MDA) as a lipid peroxidation marker. Wiad Lek 57(9-10):453–455.

884 [80] Chattopadhyay, T., Maniyadath, B., Bagul, H.P., Chakraborty, A., Shukla, N.,
885 Budnar, S., et al., 2020. Spatiotemporal gating of SIRT1 functions by
886 O-GlcNAcylation is essential for liver metabolic switching and prevents
887 hyperglycemia. Proceedings of the National Academy of Sciences of the United States
888 of America 117(12):6890–6900.
889

Figure legends

Figure 1.

***Ogt* knockout exacerbated muscle and mitochondrial damage induced by cold exposure.**

(A) Western blotting using OGT and O-GlcNAc antibodies, Tubulin serves as the loading control. Autophagy-related protein expression in muscle total extract and mitophagy-related protein expression in mitochondrial extract. After cold exposure treatment, fresh skeletal muscle tissues of four groups (wild type group, wild type + cold group, *Ogt* mKO group, *Ogt* mKO + cold group) were collected and prepared into tissue sections, which were stained by (B) Masson staning and (C) β-Galactosidase staining. (D) The mouse skeletal muscle was prepared into ultrathin sections, and the structure was observed by transmission electron microscope.

Figure 2.

***Ogt* knockout exacerbated autophagy and mitophagy by cold exposure.**

(A) After cold exposure treatment, fresh skeletal muscle tissues of four groups (wild type group, wild type + cold group, *Ogt* mKO group, *Ogt* mKO + cold group) were collected and prepared into total extract, western blotting of total muscle extract using P62, Beclin1, ATG5, LC3 and tubulin antibodies. Data are represented as mean ± SD, statistical analysis was performed by two-way ANOVA. *: $P < 0.05$; **: $P < 0.01$; ***: $P < 0.001$. (B) After cold exposure treatment, fresh skeletal muscle tissues of four groups (wild type group, wild type + cold group, *Ogt* mKO group, *Ogt* mKO + cold

group) were collected and prepared into mitochondria extract, western blotting of total muscle extract using PINK1, Parkin, DRP1, MFN1 and VDAC antibodies. Data are represented as mean ± SD, statistical analysis was performed by two-way ANOVA. *: $P < 0.05$; **: $P < 0.01$; ***: $P < 0.001$. (C) Fresh skeletal muscle tissue from each group was collected, prepared into tissue sections, and stained with DHE dye for reactive oxygen species (ROS). (D) After cold exposure treatment, fresh skeletal muscle tissue was collected to detect the content of MDA. n = 3/group. Data are represented as mean ± SD, statistical analysis was performed by two-way ANOVA. *: $P < 0.05$; **: $P < 0.01$; ***: $P < 0.001$. (E) Fresh skeletal muscle tissue was prepared into ultrathin sections and mitochondrial function was tested by cellular mitochondrial pressure test, which including basal respiration, ATP production, maximum respiration and spare respiratory. n = 3/group. Data are represented as mean ± SD, statistical analysis was performed by two-way ANOVA. *: $P < 0.05$; **: $P < 0.01$; ***: $P < 0.001$.

Figure 3.

Cold exposure enhanced protein acetylation through downregulating SIRT1.

(A) After cold exposure treatment, fresh skeletal muscle tissues of four groups (wild type group, wild type + cold group, *Ogt* mKO group, *Ogt* mKO + cold group) were collected and prepared into total extract and nucleus extract, western blotting of total muscle extract using acetylated-lysine, SIRT1, Acetyl-FoxO1, FoxO1, and tubulin antibodies. $H3^{K9}$ and H3 expression in muscle nucleus extract. n = 3/group. Data are

represented as mean ± SD, statistical analysis was performed by two-way ANOVA. *: $P < 0.05$; **: $P < 0.01$; ***: $P < 0.001$. (B-D) Fresh skeletal muscle tissue was collected to detect the (B) content of NAD^+, (C) SIRT1 activity, and (D) *Sirt*1 mRNA expression. n = 3/group. Data are represented as mean ± SD, statistical analysis was performed by two-way ANOVA. *: $P < 0.05$; **: $P < 0.01$; ***: $P < 0.001$.

Figure 4.

Mild hypothermia induced autophagy and mitophagy in C2C12 cells.

(A–B) After C2C12 cells were treated at 32 ℃ for 3 h, collected them and prepared into ultrahin sections, (A) ultrahin sections were stained by β-Galactosidase staining and (B) the structure was observed by transmission electron microscopy. (C) Autophagy-related protein expression in total extract and (D) mitophagy-related protein expression in mitochondria extract. n = 3/group. Data are represented as mean ± SD, statistical analysis was performed by student's t-test. Symbol [*] compared with control group. Symbol [#] compared with mild hypothermia group. *: $P < 0.05$; **:$P < 0.01$; ***: $P < 0.001$. #: $P < 0.05$; ##: $P < 0.01$; ###: $P < 0.001$.

Figure 5.

Mild hypothermia compromised mitochondrial function.

The mice skeletal muscle primary cells were isolated and cultured. After 3 h mild hypothermia treatment at 32 ℃, the skeletal muscle primary cells were collected to detect the function. (A) Staining of C2C12 cells with Mito-Tracker Red CMXRos. (B)

JC-1 staining of C2C12 cells. (C) Mitochondrial function was tested by cellular mitochondrial pressure test, which including basal respiration, ATP production, maximum respiration and spare respiratory. n = 3/group. Data are represented as mean ± SD, statistical analysis was performed by student's t-test. Symbol [*] compared with control group. Symbol [#] compared with mild hypothermia group. *: $P < 0.05$; **: $P < 0.01$; ***: $P < 0.001$. #: $P < 0.05$; ##: $P < 0.01$; ###: $P < 0.001$. (D) Immunocytochemical staining of Nrf2 protein in C2C12 cells. (E) Flow cytometry showing ROS production in C2C12 cells. (F) MDA content. n = 3/group. Data are represented as mean ± SD, statistical analysis was performed by student's t-test. Symbol [*] compared with control group. Symbol [#] compared with mild hypothermia group. *: $P < 0.05$; **: $P < 0.01$; ***: $P < 0.001$. #: $P < 0.05$; ##: $P < 0.01$; ###: $P < 0.001$.

Figure 6.

Mild hypothermia increased acetylation through SIRT1 inhibition.

(A–C) After 3h mild hypothermia treatment at 32 ℃, the C2C12 cells were collected to detect (A) NAD^+ content, (B) SIRT1 activity, and (C) *Sirt*1 mRNA expression. n = 3/group. Data are represented as mean ± SD, statistical analysis was performed by student's t-test. Symbol [*] compared with control group. Symbol [#] compared with mild hypothermia group. *: $P < 0.05$; **: $P < 0.01$; ***: $P < 0.001$. #: $P < 0.05$; ##: $P < 0.01$; ###: $P < 0.001$. (D) Expression level of O-GlcNAcylation, acetylated-lysine and AC-FoxO1K262/k265/k274 protein. n = 3/group. Data are represented as mean ±

SD, statistical analysis was performed by student's t-test. Symbol [*] compared with control group. Symbol [#] compared with mild hypothermia group. *: $P < 0.05$; **: $P < 0.01$; ***: $P < 0.001$. #: $P < 0.05$; ##: $P < 0.01$; ###: $P < 0.001$. (E) After 3 h mild hypothermia treatment at 32 ℃, the C2C12 cells were collected to prepared into total extract. Add 30 μL agarose succinylated wheat germ agglutinin to total extract, incubated overnight at 4 ℃, and the glycosylated protein is combined with agarose succinylated wheat germ agglutinin. The next day, the supernatant was discarded after centrifugation, washed three times with PBS, added with loading bufffer and boiled, and the supernatant was taken for western blotting. Western blotting using SIRT1 and O-GlcNAc antibodies.

Figure 7.

Overexpressing SIRT1 ameliorated cold stress syndrome.

After the corresponding treatment, C2C12 cells were collected and prepared into total extract, mitochondria extract and nucleus extract. (A) Autophagy-related protein expression in total extract. (B) Mitophagy-related protein expression in mitochondria extract. (C) Nrf2 and $H3^{K9}$ protein expression in nucleus extract. n = 3/group. Data are represented as mean ± SD, statistical analysis was performed by student's t-test. Symbol [*] compared with hypothermia group. Symbol [#] compared with mild hypothermia group. SIRT1+mild hypothermia group. *: $P < 0.05$; **: $P < 0.01$; ***: $P < 0.001$. #: $P < 0.05$; ##: $P < 0.01$; ###: $P < 0.001$. (D) Nrf2 protein localization was detected by immunofluorescence staining. (E) ROS was detected by flow

cytometry. (F) MDA content. n = 3/group. Data are represented as mean ± SD, statistical analysis was performed by student's t-test. Symbol [*] compared with hypothermia group. Symbol [#] compared with mild hypothermia group. SIRT1+ mild hypothermia group. *: $P < 0.05$; **: $P < 0.01$; ***: $P < 0.001$. #: $P < 0.05$; ##: $P < 0.01$; ###: $P < 0.001$.

Figure 8.

SIRT1 overexpression rescued cold-induced mitochondrial defect.

After the corresponding treatment, C2C12 cells were collected and detected the function. (A) Staining of C2C12 cells with Mito-Tracker Red CMXRos. (B) JC-1 staining of C2C12 cells. (C) Mitochondrial function was tested by cellular mitochondrial pressure test, which including basal respiration, ATP production, maximum respiration and spare respiratory. n = 3/group. Data are represented as mean ± SD, statistical analysis was performed by student's t-test. Symbol [*] compared with hypothermia group. Symbol [#] compared with mild hypothermia group. SIRT1+mild hypothermia group. *: $P < 0.05$; **: $P < 0.01$; ***: $P < 0.001$. #: $P < 0.05$; ##: $P < 0.01$; ###: $P < 0.001$.

Figure 9.

Graphical abstract.

The expression of SIRT1 was inhibited and the level of deacetylation decreased in mice under cold exposure, meanwhile, SIRT1-FoxO1 pathway was activated,

resulting in increased acetylation of histones and oxidative stress, recruitment of more Nrf2 into the nucleus, resulting in damage to the structure and function of mitochondria, resulting in excessive mitophagy and macroautophagy in mouse skeletal muscle. At the same time, this research demonstrated that the O-GlcNAcylation of SIRT1 can alleviate the imbalance of mice skeletal muscle mitochondrial homeostasis caused by cold exposure, which was a protective mechanism of the body.

Supplementary Figure 1.

Statistics of autophagy and mitophagy-related proteins in C2C12 cells after mild hypothermia treatment for different durations.

C2C12 cells were cultured at 32 ℃ for 3 h, 6 h and 9 h, respectively, and C2C12 cells were collected to prepare total extract and mitochondria extract. The expression levels of autophagy and mitophagy-related proteins in C2C12 cells were detected by western blotting. n = 3/group. Data are represented as mean ± SD, statistical analysis was performed by one-way ANOVA. Symbol [*] compared with mild hypothermia group. *: $P < 0.05$; **: $P < 0.01$; ***: $P < 0.001$.

Figures

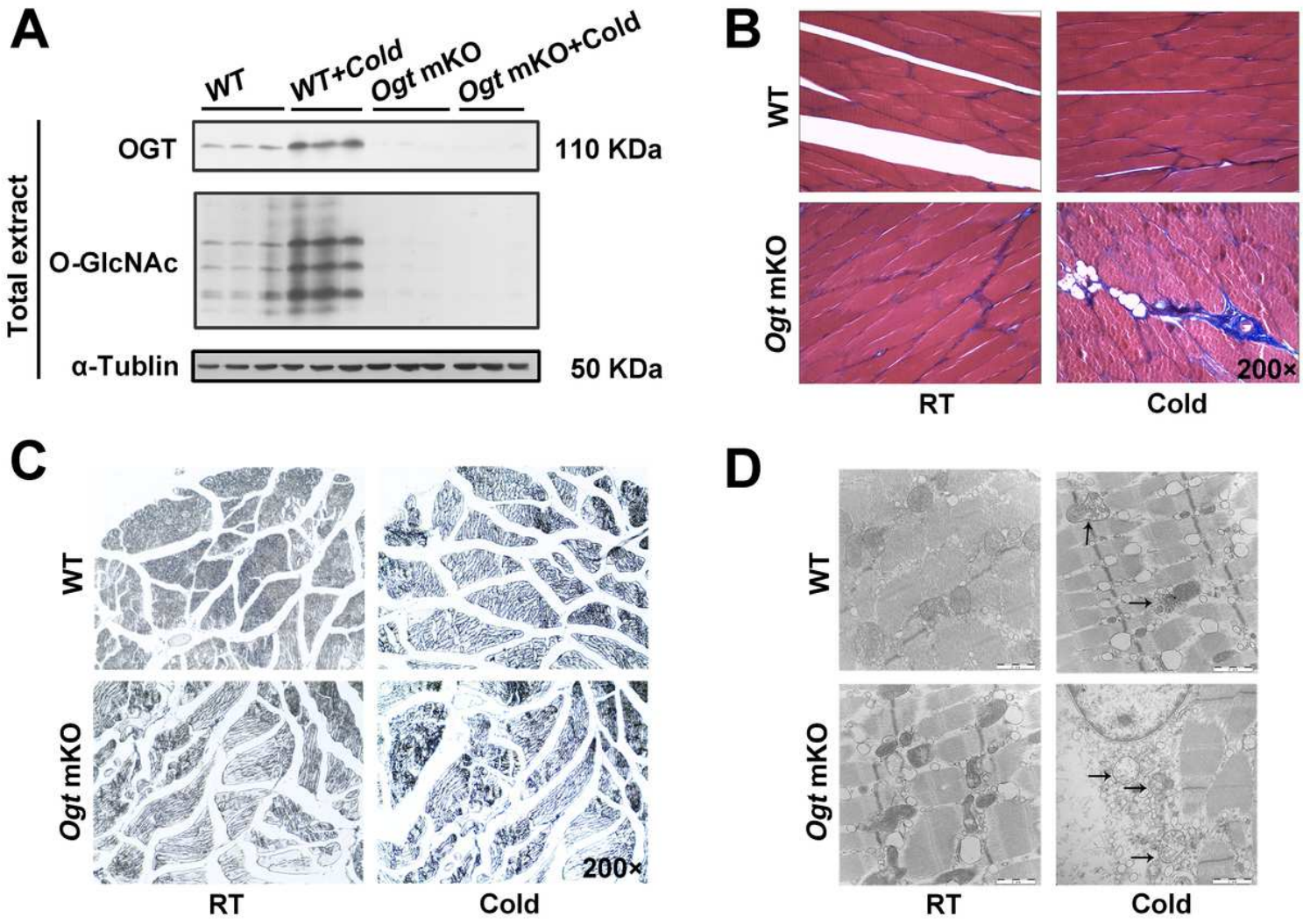

Figure 1

***Ogt* knockout exacerbated muscle and mitochondrial damage induced by cold exposure.**

(A) Western blotting using OGT and O-GlcNAc antibodies, Tubulin serves as the loading control. Autophagy-related protein expression in muscle total extract and mitophagy-related protein expression in mitochondrial extract. After cold exposure treatment, fresh skeletal muscle tissues of four groups (wild type group, wild type + cold group, *Ogt* mKO group, *Ogt* mKO + cold group) were collected and prepared into tissue sections, which were stained by (B) Masson staning and (C) β-Galactosidase staining. (D) The mouse skeletal muscle was prepared into ultrathin sections, and the structure was observed by transmission electron microscope.

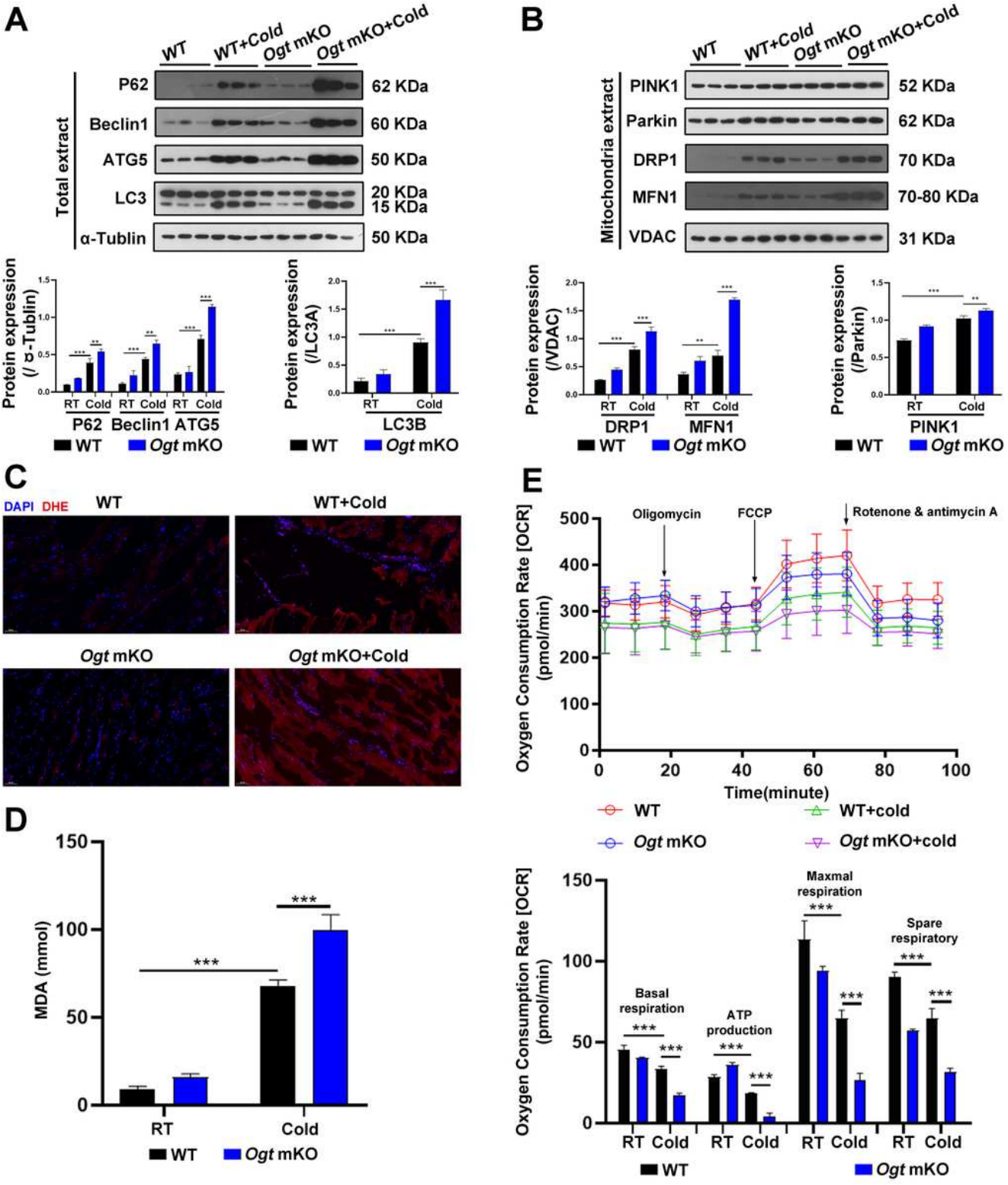

Figure 2

***Ogt* knockout exacerbated autophagy and mitophagy by cold exposure.**

(A) After cold exposure treatment, fresh skeletal muscle tissues of four groups (wild type group, wild type + cold group, *Ogt* mKO group, *Ogt* mKO + cold group) were collected and prepared into total extract, western blotting of total muscle extract using P62, Beclin1, ATG5, LC3 and tubulin antibodies. Data are

represented as mean ± SD, statistical analysis was performed by two-way ANOVA. *: $P < 0.05$; **: $P < 0.01$; ***: $P < 0.001$. (B) After cold exposure treatment, fresh skeletal muscle tissues of four groups (wild type group, wild type + cold group, *Ogt* mKO group, *Ogt* mKO + cold group) were collected and prepared into mitochondria extract, western blotting of total muscle extract reactive oxygen species (ROS). (D) After cold exposure treatment, fresh skeletal muscle tissue was collected to detect the content of MDA using PINK1, Parkin, DRP1, MFN1 and VDAC antibodies. Data are represented as mean ± SD, statistical analysis was performed by two-way ANOVA. *: $P < 0.05$; **: $P < 0.01$; ***: $P < 0.001$. (C) Fresh skeletal muscle tissue from each group was collected, prepared into tissue sections, and stained with DHE dye for. n = 3/group. Data are represented as mean ± SD, statistical analysis was performed by two-way ANOVA. *: $P < 0.05$; **: $P < 0.01$; ***: $P < 0.001$. (E) Fresh skeletal muscle tissue was prepared into ultrathin sections and mitochondrial function was tested by cellular mitochondrial pressure test, which including basal respiration, ATP production, maximum respiration and spare respiratory. n = 3/group. Data are represented as mean ± SD, statistical analysis was performed by two-way ANOVA. *: $P < 0.05$; **: $P < 0.01$; ***: $P < 0.001$.

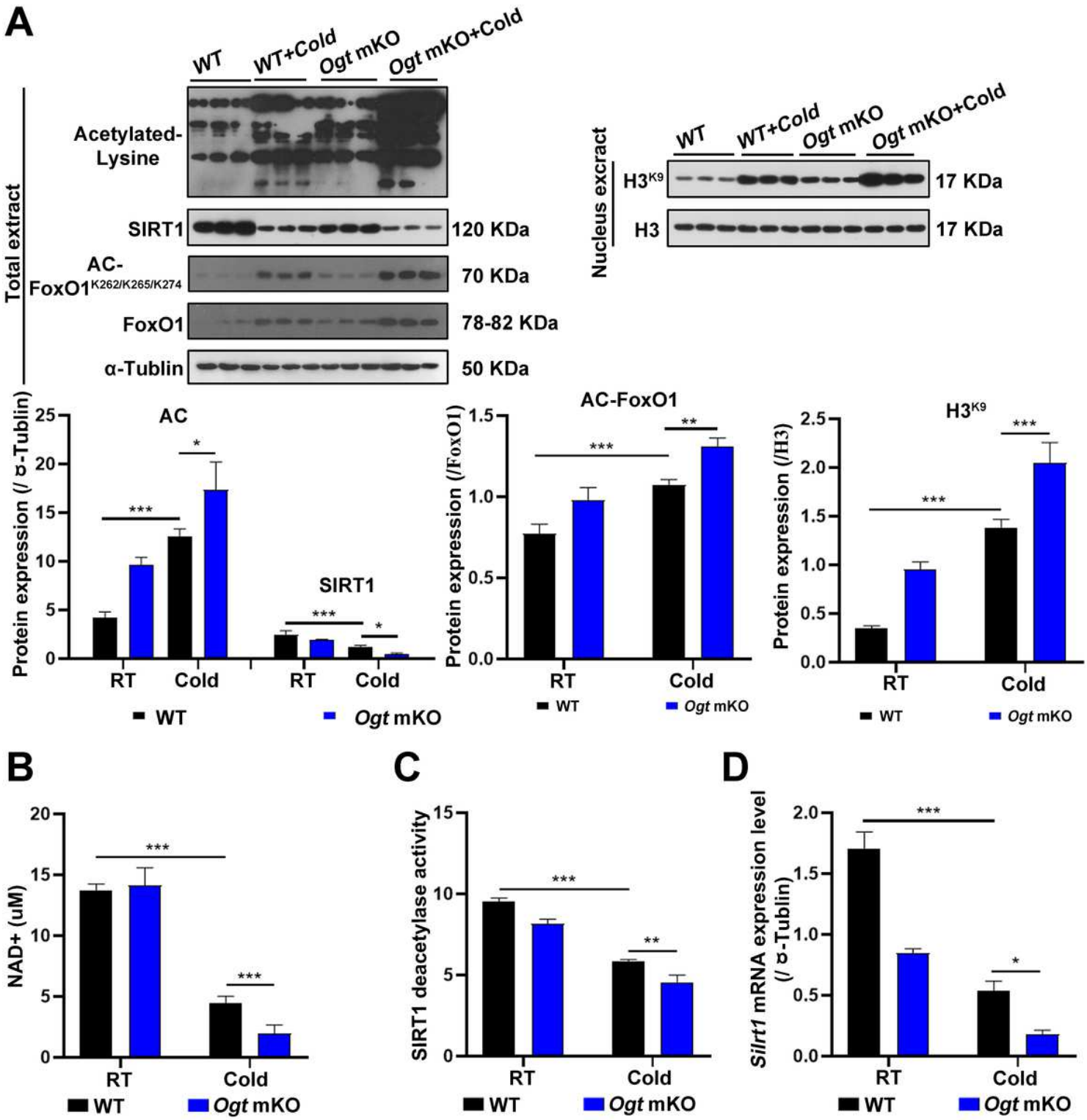

Figure 3

Cold exposure enhanced protein acetylation through downregulating SIRT1.

(A) After cold exposure treatment, fresh skeletal muscle tissues of four groups (wild type group, wild type + cold group, *Ogt* mKO group, *Ogt* mKO + cold group) were collected and prepared into total extract and nucleus extract, western blotting of total muscle extract using acetylated-lysine, SIRT1, Acetyl-FoxO1, FoxO1, and tubulin antibodies. $H3^{K9}$ and H3 expression in muscle nucleus extract. n = 3/group. Data are

represented as mean ± SD, statistical analysis was performed by two-way ANOVA. *: $P < 0.05$; **: $P < 0.01$; ***: $P < 0.001$. (B-D) Fresh skeletal muscle tissue was collected to detect the (B) content of NAD+, (C) SIRT1 activity, and (D) *Sirt*1 mRNA expression. n = 3/group. Data are represented as mean ± SD, statistical analysis was performed by two-way ANOVA. *: $P < 0.05$; **: $P < 0.01$; ***: $P < 0.001$.

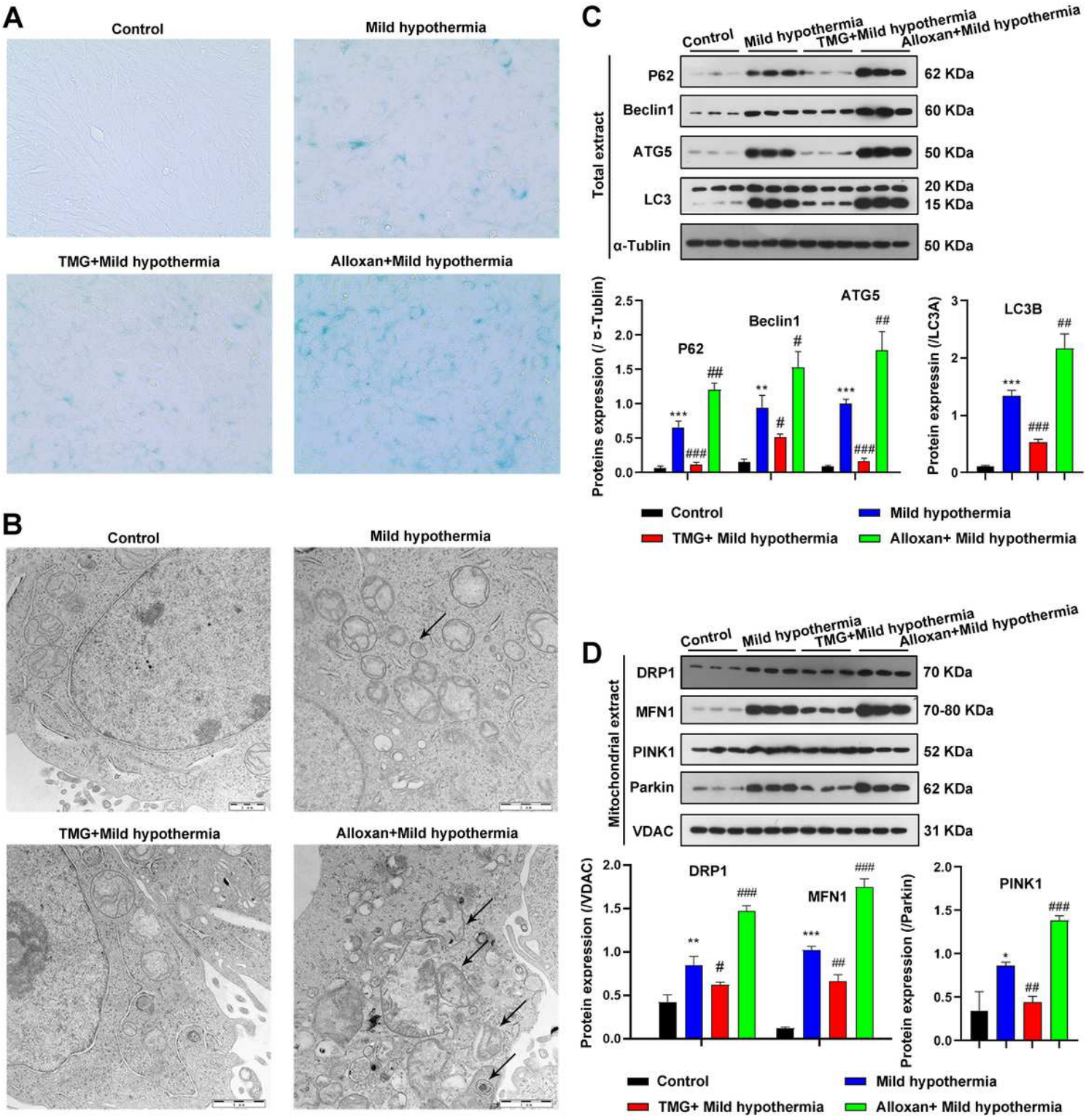

Figure 4

Mild hypothermia induced autophagy and mitophagy in C2C12 cells.

(A–B) After C2C12 cells were treated at 32 ℃ for 3 h, collected them and prepared into ultrahin sections, (A) ultrahin sections were stained by β-Galactosidase staining and (B) the structure was observed by transmission electron microscopy. (C) Autophagy-related protein expression in total extract and (D) mitophagy-related protein expression in mitochondria extract. n = 3/group. Data are represented as mean ± SD, statistical analysis was performed by student's t-test. Symbol [*] compared with control group. Symbol [#] compared with mild hypothermia group. *: $P < 0.05$; **:$P < 0.01$; ***: $P < 0.001$. #: $P < 0.05$; ##: $P < 0.01$; ###: $P < 0.001$.

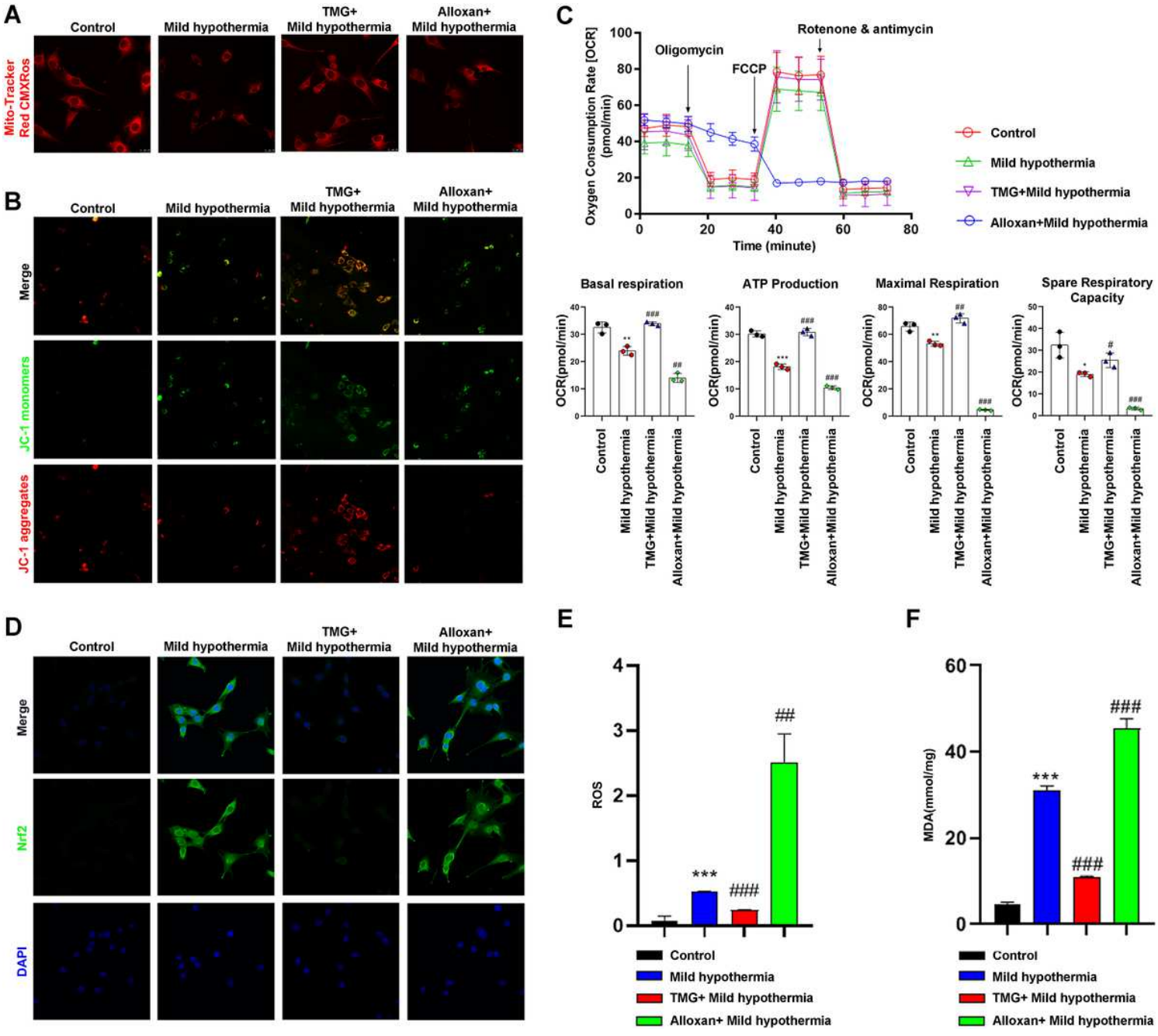

Figure 5

Mild hypothermia compromised mitochondrial function.

The mice skeletal muscle primary cells were isolated and cultured. After 3 h mild hypothermia treatment at 32 □, the skeletal muscle primary cells were collected to detect the function. (A) Staining of C2C12 cells with Mito-Tracker Red CMXRos. (B) JC-1 staining of C2C12 cells. (C) Mitochondrial function was tested by cellular mitochondrial pressure test, which including basal respiration, ATP production, maximum respiration and spare respiratory. n = 3/group. Data are represented as mean ± SD, statistical analysis was performed by student's t-test. Symbol [*] compared with control group. Symbol [#] compared with mild hypothermia group. *: $P < 0.05$; **: $P < 0.01$; ***: $P < 0.001$. #: $P < 0.05$; ##: $P < 0.01$; ###: $P < 0.001$. (D) Immunocytochemical staining of Nrf2 protein in C2C12 cells. (E) Flow cytometry showing ROS production in C2C12 cells. (F) MDA content. n = 3/group. Data are represented as mean ± SD, statistical analysis was performed by student's t-test. Symbol [*] compared with control group. Symbol [#] compared with mild hypothermia group. *: $P < 0.05$; **: $P < 0.01$; ***: $P < 0.001$. #: $P < 0.05$; ##: $P < 0.01$; ###: $P < 0.001$.

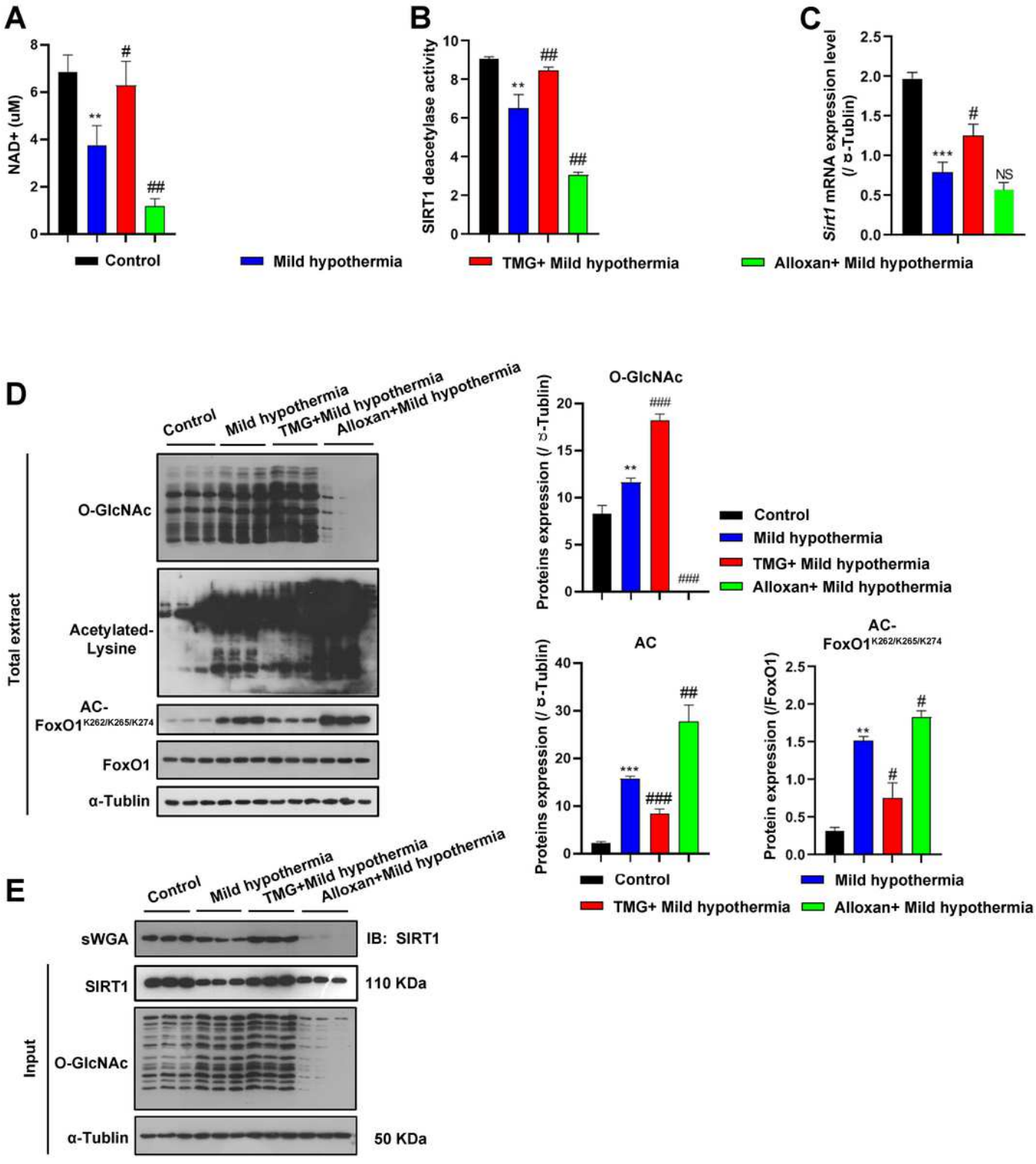

Figure 6

Mild hypothermia increased acetylation through SIRT1 inhibition.

(A–C) After 3h mild hypothermia treatment at 32 ℃, the C2C12 cells were collected to detect (A) NAD+ content, (B) SIRT1 activity, and (C) *Sirt*1 mRNA expression. n = 3/group. Data are represented as mean ± SD, statistical analysis was performed by student's t-test. Symbol [*] compared with control group.

Symbol [#] compared with mild hypothermia group. *: $P < 0.05$; **: $P < 0.01$; ***: $P < 0.001$. #: $P < 0.05$; ##: $P < 0.01$; ###: $P < 0.001$. (D) Expression level of O-GlcNAcylation, acetylated-lysine and AC-FoxO1K262/k265/k274 protein. n = 3/group. Data are represented as mean ± SD, statistical analysis was performed by student's t-test. Symbol [*] compared with control group. Symbol [#] compared with mild hypothermia group. *: $P < 0.05$; **: $P < 0.01$; ***: $P < 0.001$. #: $P < 0.05$; ##: $P < 0.01$; ###: $P < 0.001$. (E) After 3 h mild hypothermia treatment at 32 □, the C2C12 cells were collected to prepared into total extract. Add 30 μL agarose succinylated wheat germ agglutinin to total extract, incubated overnight at 4 □, and the glycosylated protein is combined with agarose succinylated wheat germ agglutinin. The next day, the supernatant was discarded after centrifugation, washed three times with PBS, added with loading bufffer and boiled, and the supernatant was taken for western blotting. Western blotting using SIRT1 and O-GlcNAc antibodies.

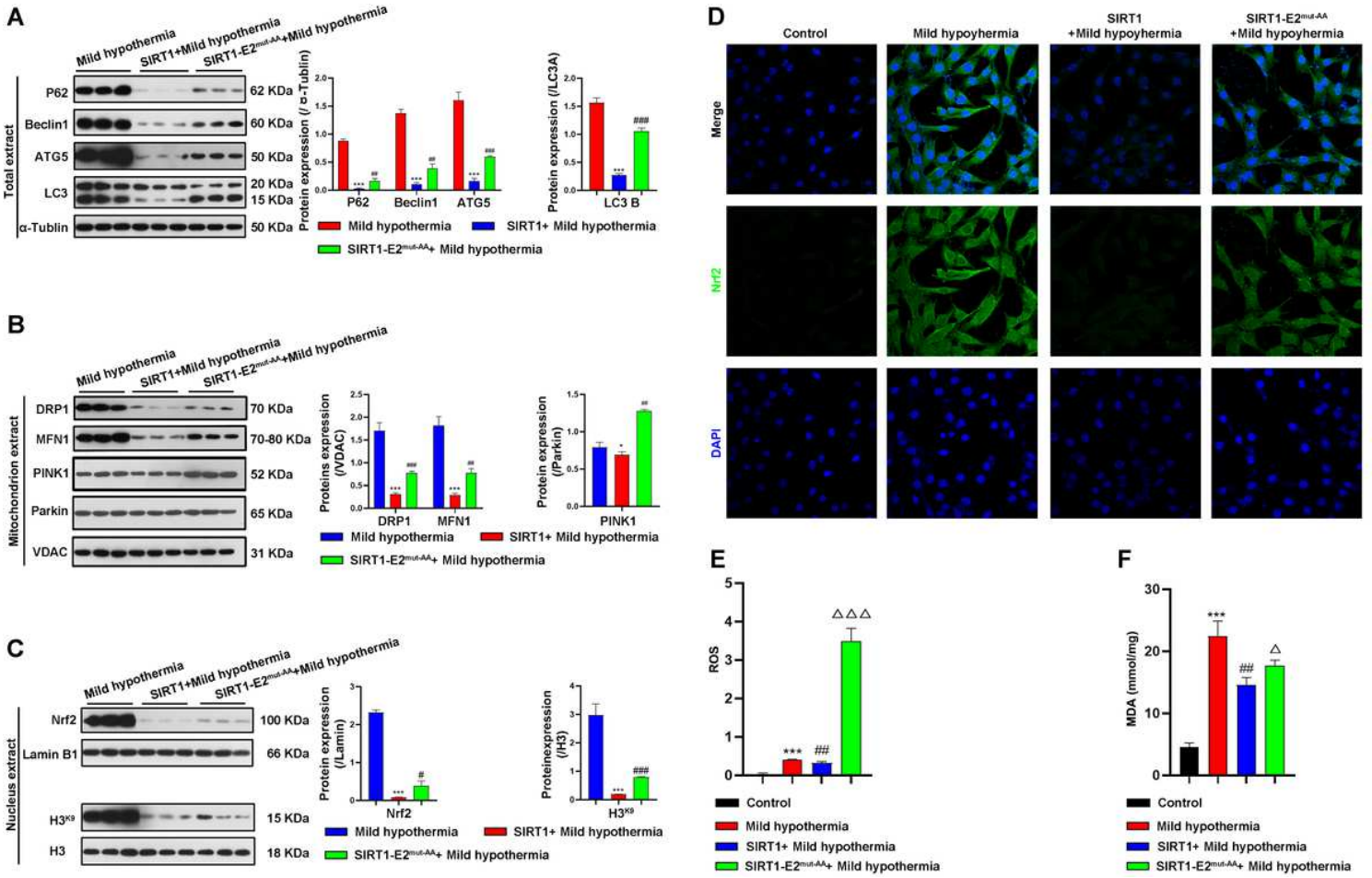

Figure 7

Overexpressing SIRT1 ameliorated cold stress syndrome.

After the corresponding treatment, C2C12 cells were collected and prepared into total extract, mitochondria extract and nucleus extract. (A) Autophagy-related protein expression in total extract. (B) Mitophagy-related protein expression in mitochondria extract. (C) Nrf2 and H3K9 protein expression in nucleus extract. n = 3/group. Data are represented as mean ± SD, statistical analysis was performed by

student's t-test. Symbol [*] compared with hypothermia group. Symbol [#] compared with mild hypothermia group. SIRT1+mild hypothermia group. *: $P < 0.05$; **: $P < 0.01$; ***: $P < 0.001$. #: $P < 0.05$; ##: $P < 0.01$; ###: $P < 0.001$. (D) Nrf2 protein localization was detected by immunofluorescence staining. (E) ROS was detected by flow cytometry. (F) MDA content. n = 3/group. Data are represented as mean ± SD, statistical analysis was performed by student's t-test. Symbol [*] compared with hypothermia group. Symbol [#] compared with mild hypothermia group. SIRT1+ mild hypothermia group. *: $P < 0.05$; **: $P < 0.01$; ***: $P < 0.001$. #: $P < 0.05$; ##: $P < 0.01$; ###: $P < 0.001$.

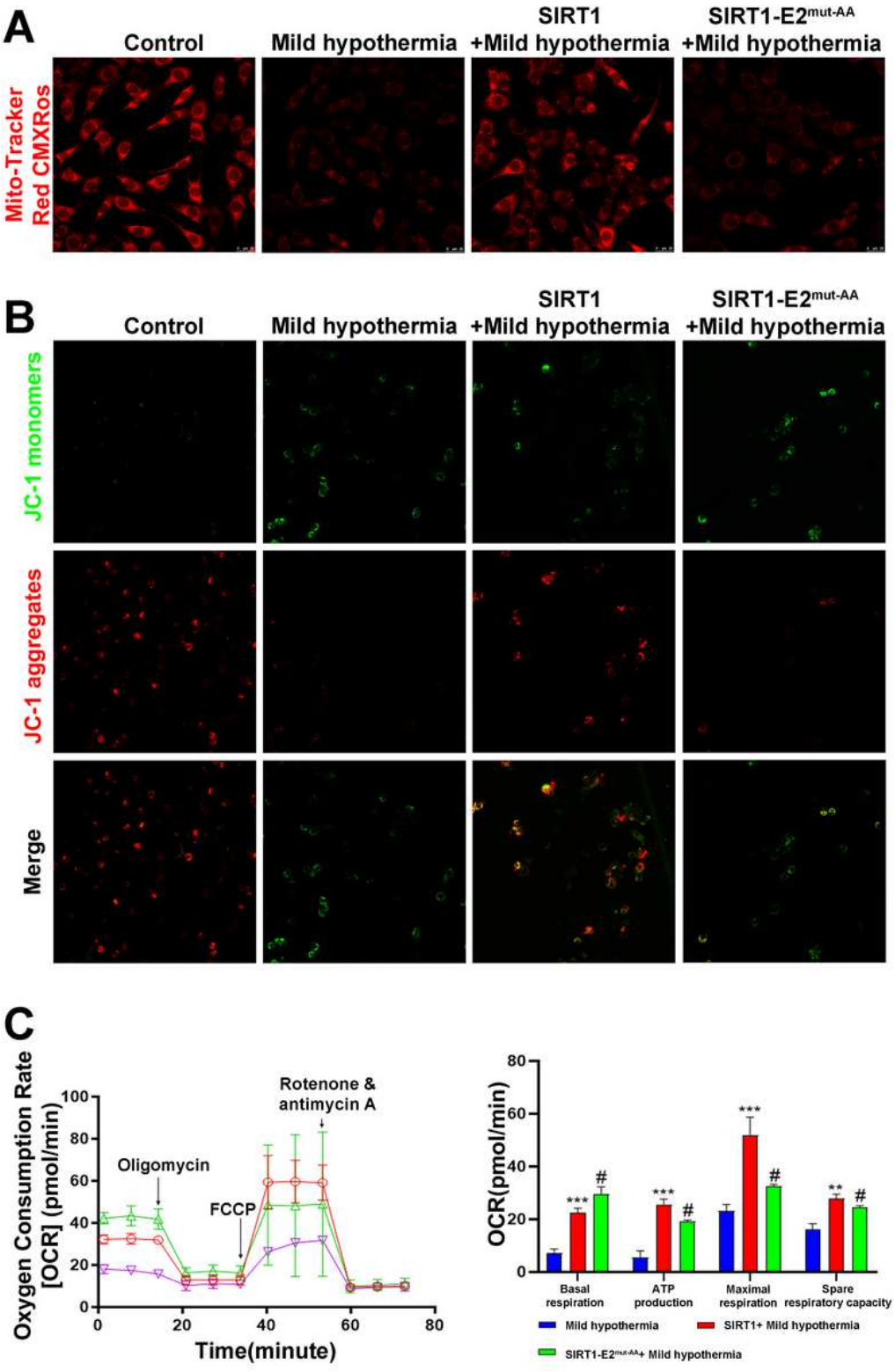

Figure 8

SIRT1 overexpression rescued cold-induced mitochondrial defect.

After the corresponding treatment, C2C12 cells were collected and detected the function. (A) Staining of C2C12 cells with Mito-Tracker Red CMXRos. (B) JC-1 staining of C2C12 cells. (C) Mitochondrial function was tested by cellular mitochondrial pressure test, which including basal respiration, ATP production, maximum respiration and spare respiratory. n = 3/group. Data are represented as mean ± SD, statistical analysis was performed by student's t-test. Symbol [*] compared with hypothermia group. Symbol [#] compared with mild hypothermia group. SIRT1+mild hypothermia group. *: $P < 0.05$; **: $P < 0.01$; ***: $P < 0.001$. #: $P < 0.05$; ##: $P < 0.01$; ###: $P < 0.001$.

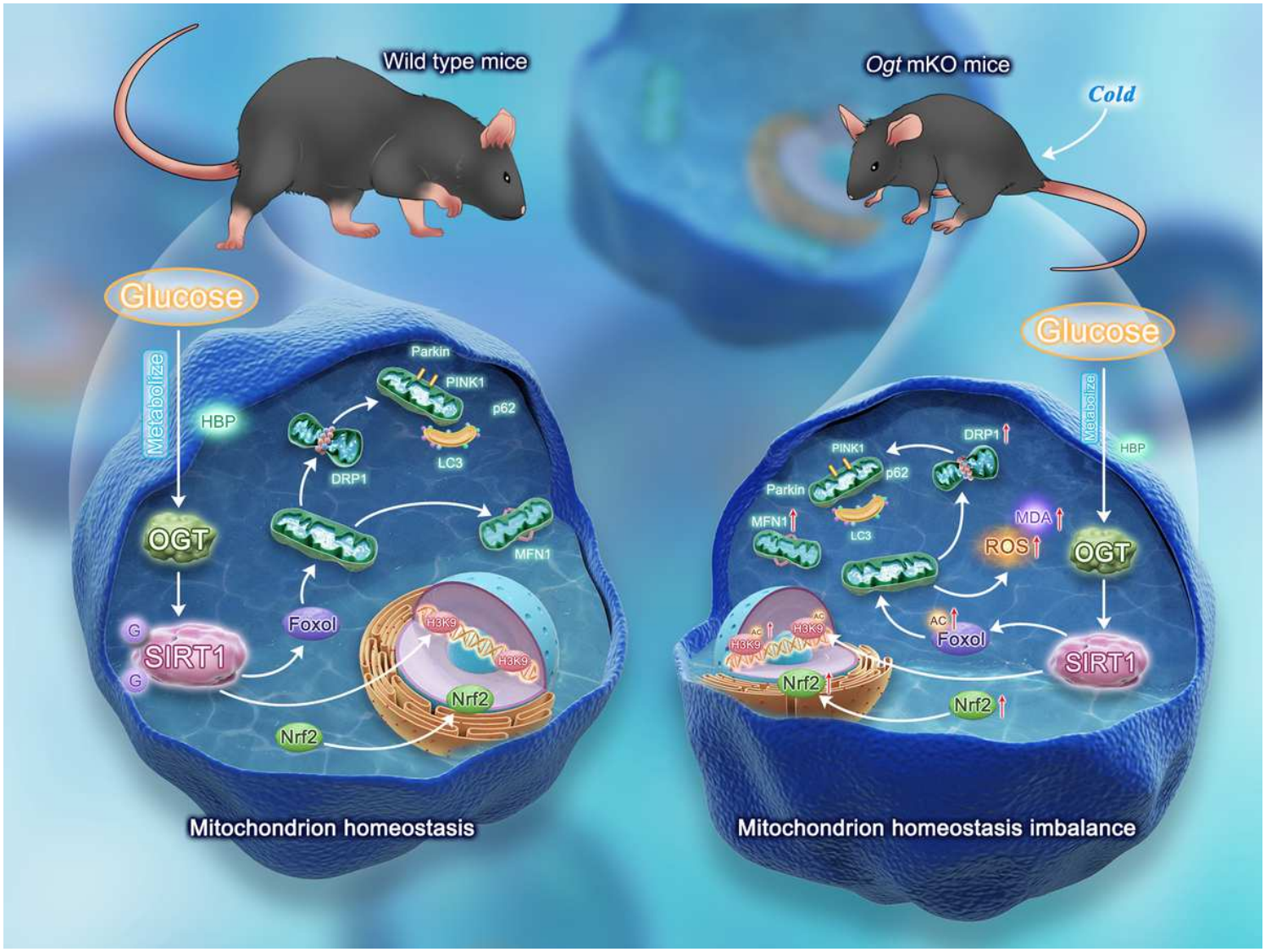

Figure 9

Graphical abstract. The expression of SIRT1 was inhibited and the level of deacetylation decreased in mice under cold exposure, meanwhile, SIRT1-FoxO1 pathway was activated, resulting in increased acetylation of histones and oxidative stress, recruitment of more Nrf2 into the nucleus, resulting in

damage to the structure and function of mitochondria, resulting in excessive mitophagy and macroautophagy in mouse skeletal muscle. At the same time, this research demonstrated that the O-GlcNAcylation of SIRT1 can alleviate the imbalance of mice skeletal muscle mitochondrial homeostasis caused by cold exposure, which was a protective mechanism of the body.

Supplementary Files

This is a list of supplementary files associated with this preprint. Click to download.

- SupplementaryFigure1.tif